ACS Photonics

Perspective

Cite This: ACS Photonics 2018, 5, 3896−3915

pubs.acs.org/journal/apchd5

Radiative Heat Transfer

Juan Carlos Cuevas*,† and Francisco J. García-Vidal†,‡

†Departamento de Física Teórica de la Materia Condensada and Condensed Matter Physics Center (IFIMAC), Universidad Autónoma de Madrid, 28049 Madrid, Spain

‡Donostia International Physics Center (DIPC), 20018 Donostia/San Sebastián, Spain

ABSTRACT: Thermal radiation is one of the most universal physical phenomena, and its study has played a key role in the history of modern physics. Our understanding of this subject has been traditionally based on Planck's law, which in particular sets limits on the amount of thermal radiation that can be emitted or exchanged. However, recent advances in the field of radiative heat transfer have defied these limits, and a plethora of novel thermal phenomena have been discovered that in turn hold the promise to have an impact in technologies that make use of thermal radiation. Here we review the rapidly growing field of radiative heat transfer, paying special attention to the remaining challenges and identifying future research directions. In particular, we focus on the recent work on near-field radiative heat transfer, including (i) experimental advances, (ii) theoretical proposals to tune, actively control, and manage near-field thermal radiation, and (iii) potential applications. We also review the recent progress in the control of thermal emission of an object, with special emphasis in its implications for energy applications, and in the comprehension of far-field radiative heat transfer. Heat is becoming the new light, and its understanding is opening many new research lines with great potential for applications.

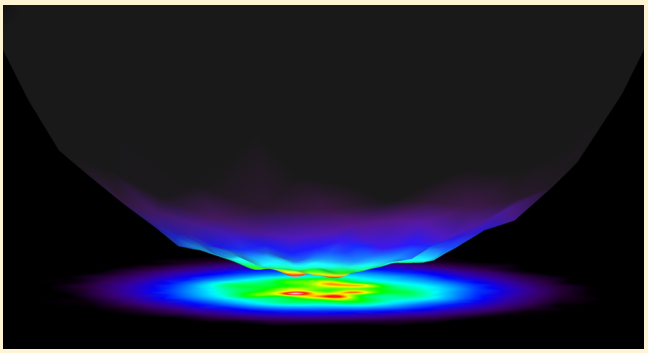

KEYWORDS: *thermal radiation, radiative heat transfer, near-field thermal radiation, super-Planckian radiative heat transfer, thermophotovoltaics*

Thermal radiation is a ubiquitous physical phenomenon, and its comprehension is of great importance for many different areas of science and engineering.[1−3] For a long time, it was believed that this phenomenon was fairly well understood, and the topic of radiative heat transfer was basically considered textbook material. Our understanding of thermal radiation is still largely based on Planck's law, which tells us that a blackbody (an object that absorbs all of the radiation that hits it) emits thermal radiation following a universal broad-band distribution that depends only on the body's temperature.[4] Planck's law describes in a unified manner the different classical thermal radiation laws, and in particular, it sets an upper limit for the radiative heat transfer (RHT) between bodies at different temperatures. However, Planck's law was derived under the assumption that all of the dimensions involved in a thermal problem are much longer than the thermal wavelength λ_{th} (∼10 μm at room temperature), and therefore, it is expected to fail in a variety of situations. Thus, for instance, Planck's law is unable to describe the RHT between objects separated by distances smaller than λ_{th}.[5−7] In this near-field regime, the RHT is dominated by evanescent waves, which are not considered in Planck's law, and the Planckian limit can be greatly overcome by bringing objects sufficiently close. This phenomenon was first predicted in the early 1970s[8] by making use of the theory of fluctuational electrodynamics,[9,10] and its experimental verification in recent years has boosted the field of thermal radiation.[11−34] Moreover, this fact has triggered the hope that near-field RHT may have an impact in different technologies such as heat-assisted magnetic recording,[35,36] thermal lithography,[37] scanning thermal microscopy,[38−40] coherent thermal sources,[41,42] near-field-based thermal management,[21,43−45] thermophotovoltaics,[46−59] and other energy conversion devices.[60−62]

Planck's law, which is based on ray optics and disregards diffraction-like phenomena, is also expected to fail in the far-field regime when some of the characteristic dimensions of an object are smaller than λ_{th}. Thus, for instance, it has been shown that nanophotonic structures, where at least one of the structural features is at subwavelength scale, can have thermal radiation properties that differ drastically from those of conventional thermal emitters.[63] In particular, it has been demonstrated that one can tailor a variety of properties of the far-field thermal emission of an object, including its spectral distribution,[64−67] its polarization,[42,68−70] and its angular dependence.[42,71−77] These advances have led in turn to the development or improvement of energy applications such as daytime passive radiative cooling,[78−85] thermal radiative

Received: July 26, 2018
Revised: September 19, 2018
Accepted: September 19, 2018
Published: September 19, 2018

DOI: 10.1021/acsphotonics.8b01031
ACS Photonics 2018, 5, 3896−3915

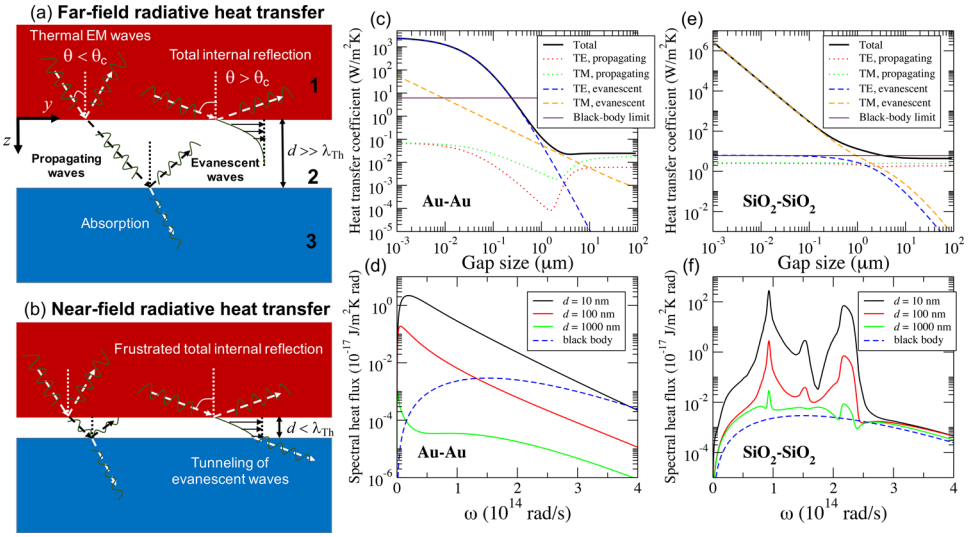

Figure 1. (a) Far-field radiative heat transfer between two infinite parallel plates (media 1 and 3) separated by a vacuum gap (medium 2). In this case, the gap size, d, is much larger than the thermal wavelength, λ_{th}, and the two plates can exchange heat only via propagating waves. The evanescent waves generated in the vacuum gap by total internal reflection are not able to reach the second plate and do not contribute to the heat transfer in this regime. (b) When the gap size is smaller than λ_{th}, tunneling of evanescent waves can make a significant contribution to the radiative heat transfer, and in this way the Planckian limit can be greatly overcome in this near-field regime. (c) Heat transfer coefficient at room temperature (300 K) as a function of the gap size for two infinite parallel plates made of Au. The different lines correspond to the total contribution (black solid line) and the contributions of propagating and evanescent waves for transverse electric (TE) and transverse magnetic (TM) polarizations. The horizontal line shows the result for two blackbodies (6.124 W m^{-2} K^{-1}). (d) Spectral heat flux (or conductance per unit area and frequency) as a function of the radiation frequency corresponding to (c). The solid lines correspond to three different values of the gap size in the near-field regime, while the blue dashed line is the result for two blackbodies. (e, f) Same as in (c, d) for SiO_2.

textiles,[86−94] radiative cooling of solar cells,[95−97] and thermophotovoltaic cells.[98,99] On a more fundamental level, it has also been shown that basic laws like Kirchhoff's law, which establishes the equality of the emissivity and absorptivity of an object and was believed to be universally valid, can actually be violated in nonreciprocal systems.[100] Another fundamental question that has attracted a lot of attention is the possibility of overcoming the far-field limits set by Planck's law in the context of the thermal emission of an object and RHT between objects. Although it has become clear that the Planckian limits cannot be overcome with extended structures (regardless of whether they have subwavelength structural features),[101] nothing prevents beating those limits in the case of objects with dimensions smaller than λ_{th}.[10,102] In fact, it has been suggested that the far-field thermal emission of a single object can be super-Planckian,[101,103−105] but in practice this is very difficult to achieve, and this phenomenon has never been observed. However, in the context of RHT it has been predicted very recently that the Planckian limit can be largely surpassed in the far-field regime,[106] i.e., when the separation of the objects is larger than λ_{th}. In particular, it has been shown that the far-field RHT between micron-sized dielectric devices can overcome the blackbody limit by several orders of magnitude if their thickness is much smaller than λ_{th}. It has also been shown that this violation can become much more dramatic in the case of the far-field RHT between coplanar two-dimensional (2D) materials such as graphene and black phosphorus.[107] These recent results illustrate the dramatic failure of the classical theory to predict the RHT between micro- and nanodevices, even in the far-field regime.

In this Perspective, we review the re-emerging field of radiative heat transfer, a topic that has returned to research laboratories and holds the promise to have an impact in a number of thermal technologies and to lead to a variety of unforeseen applications. In particular, we shall review the recent progress in the understanding of RHT in both the near- and far-field regimes, with a special emphasis on the open problems and future research directions.

NEAR-FIELD RADIATIVE HEAT TRANSFER: THE CONCEPT

The central idea that has revolutionized the field of radiative heat transfer in the last two decades is the fact that when two objects are separated by a distance smaller than λ_{th}, the radiative heat flux can be greatly enhanced as a result of the contribution of tunneling of evanescent waves (Figure 1a,b). This additional near-field contribution, which plays no role in the far-field regime (where objects are separated by distances much larger than λ_{th}), makes it possible to overcome the limit set by Planck's law by bringing objects sufficiently close. A convenient way to understand the concept of near-field radiative heat transfer (NFRHT) is by recalling the seminal result obtained by Polder and Van Hove[8] for the radiative heat transfer between two infinite parallel plates. This result was obtained with the help of the theory of fluctuational electrodynamics, which will be reviewed in the next section.

Let us consider two infinite parallel plates made of optically isotropic materials that are separated by a vacuum gap of width d (Figure 1a). We shall refer to the upper plate as medium 1, the vacuum gap as medium 2, and the lower plate as medium 3. The net radiative power per unit area exchanged between the parallel plates (which are at temperatures T_1 and T_3, respectively, with $T_1 > T_3$) is given by[8]

$$Q = \int_0^\infty \frac{d\omega}{2\pi} [\Theta(\omega, T_1) - \Theta_3(\omega, T_3)] \int_0^\infty \frac{dk}{2\pi} k\tau(\omega, k, d) \quad (1)$$

DOI: 10.1021/acsphotonics.8b01031
ACS Photonics 2018, 5, 3896−3915

where $\Theta(\omega, T_i) = \hbar\omega/[\exp(\hbar\omega/k_B T_i) - 1]$, T_i is the absolute temperature of medium i, ω is the radiation frequency, $k = \sqrt{k_x^2 + k_y^2}$ is the magnitude of the wave vector parallel to the surface planes (see the coordinate system in Figure 1a), and $\tau(\omega, k, d)$ is the total transmission probability of the electromagnetic waves. In the case of isotropic materials, this total transmission can be written as $\tau(\omega, k, d) = \tau_s(\omega, k, d) + \tau_p(\omega, k, d)$, where the contributions of s- and p-polarized waves (or alternatively, transverse electric (TE) and transverse magnetic (TM) waves) are given by

$$\tau_{\alpha=s,p}(\omega, k, d) = \begin{cases} (1 - |r_{21}^{\alpha}|^2)(1 - |r_{23}^{\alpha}|^2)/|D_{\alpha}|^2, & k < \omega/c \\ 4\,\mathrm{Im}\{r_{21}^{\alpha}\}\,\mathrm{Im}\{r_{23}^{\alpha}\}e^{-2|q_2|d}/|D_{\alpha}|^2, & k > \omega/c \end{cases} \quad (2)$$

where $D_{\alpha} = 1 - r_{21}^{\alpha} r_{23}^{\alpha} e^{2iq_2 d}$, c is the speed of light, $q_2 = \sqrt{\omega^2/c^2 - k^2}$ is the z component of the wave vector in the vacuum gap, and r_{ij}^{α} are Fresnel (or reflection) coefficients, given by

$$r_{ij}^{s} = \frac{q_i - q_j}{q_i + q_j}, \qquad r_{ij}^{p} = \frac{\epsilon_j q_i - \epsilon_i q_j}{\epsilon_j q_i + \epsilon_i q_j} \quad (3)$$

where $q_i = \sqrt{\epsilon_i \omega^2/c^2 - k^2}$, in which $\epsilon_i(\omega)$ is the dielectric function of medium i.

The key issue in eq 1 is that the second integral is carried out over all possible values of k and therefore includes the contributions of both propagating waves ($k < \omega/c$) and evanescent waves ($k > \omega/c$). This latter contribution decays exponentially with the gap size (see eq 2) and becomes negligible in the far-field regime ($d \gg \lambda_{th}$). However, in the near-field regime ($d < \lambda_{th}$) the contribution of evanescent waves can become very significant, and for sufficiently small gaps it may completely dominate the heat transfer (see below). It is worth stressing that the blackbody (BB) limit is recovered from eq 1 by ignoring the evanescent waves and assuming perfect transmission for the propagating waves (for all frequencies and wave vectors). In this case, the radiative power per unit area is given by the Stefan–Boltzmann law: $Q_{BB} = \sigma(T_1^4 - T_3^4)$, where $\sigma = 5.67 \times 10^{-8}$ W m^{-2} K^{-4}.

To illustrate the impact of NFRHT, we show in Figure 1 the results for the gap dependence of the heat transfer coefficient, i.e., the linear radiative heat conductance per unit area, for two identical plates made of (c) Au and (e) SiO_2. It should be noted that in both cases the Planckian limit can be greatly overcome for sufficiently small gaps. This is particularly striking in the case of silica, where for $d = 1$ nm the heat flux is almost 5 orders of magnitude larger than in the blackbody limit. It should also be noticed that there are obvious differences between Au and SiO_2. In the case of the metal, the NFRHT is dominated by TE evanescent waves, which originate from frustrated total internal reflection waves that are evanescent in the vacuum gap but propagate inside the Au plates.[108] On the contrary, in the case of silica the NFRHT is dominated by TM evanescent waves that can be shown to stem from surface phonon polaritons (SPhPs) that result from the strong coupling of radiation with the optical phonon modes of this type of polar dielectric.[109] These surface electromagnetic waves are hybrid or cavity modes that reside in both plates and have a penetration depth that is on the order of the gap size, which implies that they are more and more confined to the surfaces as the gap is reduced.[25]

Apart from the RHT enhancement at subwavelength gaps, the near-field contribution may also result in a strong modification of the spectral heat flux (or heat conductance per unit frequency; Figure 1d,f). Thus, for instance, in the case of SiO_2, the spectral heat flux is strongly peaked at two frequencies that correspond to the frequencies of the optical modes of this polar dielectric. This is clearly at variance with the broad-band Planck distribution and is intimately related to the fact that the NFRHT in this case is dominated by SPhPs. These results illustrate the fascinating possibilities that the near field opens for the topic of thermal radiation.

THEORETICAL AND COMPUTATIONAL APPROACHES

Most of the theoretical work done on NFRHT is carried out within the framework of fluctuational electrodynamics (FE), which was developed by Rytov in the 1950s.[9,10] This is a semiclassical approach in which one assumes that the thermal radiation is generated by random, thermally activated electric currents inside the bodies. These currents vanish on average, but their correlations are given by the fluctuation–dissipation theorem.[5] Thus, the technical problem involved in the description of RHT is to find the solution of the stochastic Maxwell equations with random electric currents as radiation sources. Briefly, let us consider a system comprising two optically isotropic bodies separated by a vacuum gap, as shown in Figure 2. The RHT problem is completely specified by the

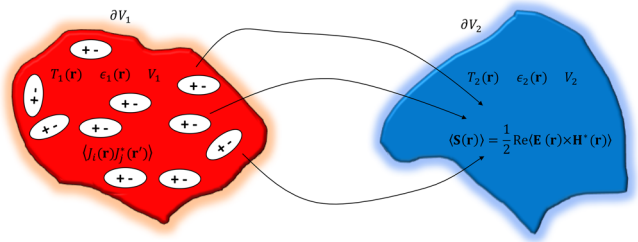

Figure 2. Fluctuational electrodynamics. Shown is a schematic of radiative heat transfer between two bodies separated by a vacuum gap. The two bodies, with volumes V_1 and V_2, are characterized by temperature profiles $T_1(\mathbf{r})$ and $T_2(\mathbf{r})$ and frequency-dependent dielectric functions $\epsilon_1(\mathbf{r})$ and $\epsilon_2(\mathbf{r})$ that may vary in space. Electromagnetic fields $\mathbf{E}$ and $\mathbf{H}$ are generated by the random currents $\mathbf{J}$ in the bodies as a result of their nonvanishing correlations given by the fluctuation–dissipation theorem.

temperature distributions $T_i(\mathbf{r})$ ($i = 1, 2$) and the relative complex dielectric functions of the materials, $\epsilon_i(\mathbf{r}, \omega)$. Working with the time-harmonic form of Maxwell's equations with the implicit $\exp(-i\omega t)$ time-dependent factors, the relevant macroscopic equations to be solved (for nonmagnetic materials) are

$$\nabla \times \mathbf{E}(\mathbf{r}, \omega) = i\omega\mu_0 \mathbf{H}(\mathbf{r}, \omega) \quad (4)$$

$$\nabla \times \mathbf{H}(\mathbf{r}, \omega) = -i\omega\epsilon_0 \epsilon(\mathbf{r}, \omega)\mathbf{E}(\mathbf{r}, \omega) + \mathbf{J}(\mathbf{r}, \omega) \quad (5)$$

where $\mathbf{E}$ and $\mathbf{H}$ are the complex electric and magnetic field vectors, $\mathbf{r}$ is the position vector, and ϵ_0 and μ_0 are the vacuum permittivity and permeability, respectively. In the second equation, the fluctuating current density distributions $\mathbf{J}(\mathbf{r}, \omega)$ within the bodies are the sources of electromagnetic heat

DOI: 10.1021/acsphotonics.8b01031
ACS Photonics 2018, 5, 3896–3915

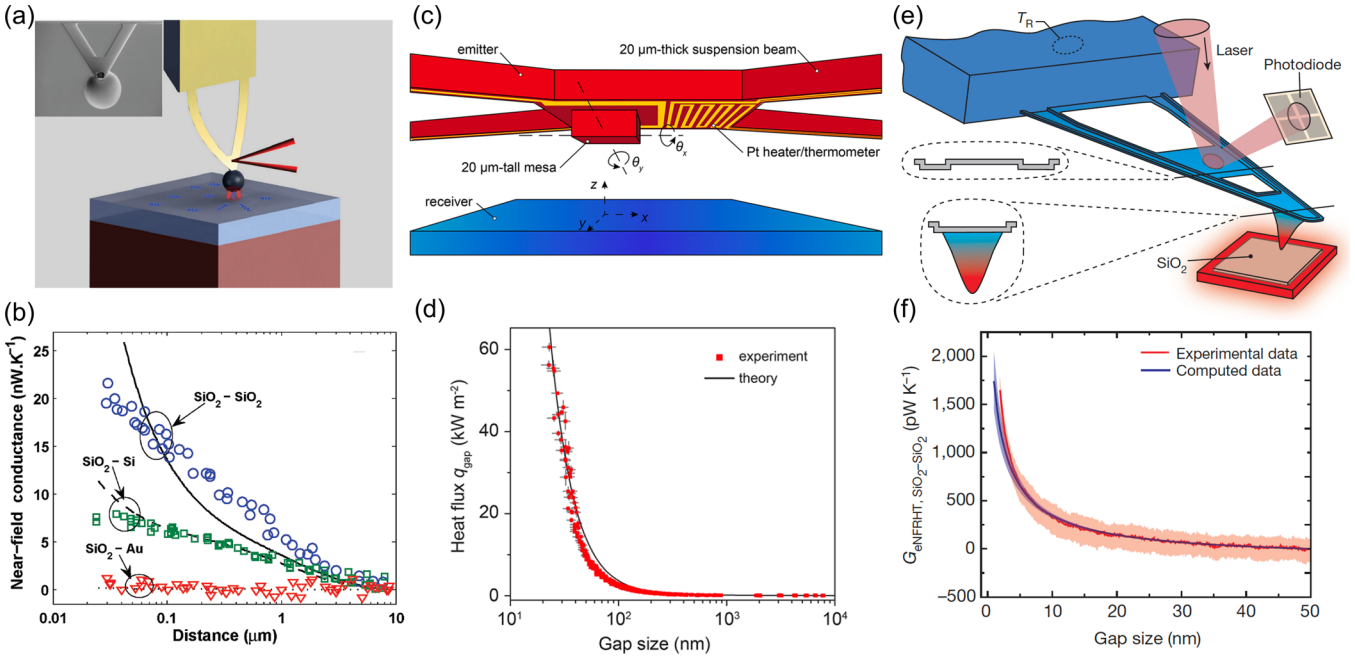

Figure 3. NFRHT measurements. (a) Schematic of the experimental setup to measure the NFRHT between a sphere and a plane using a bimaterial-cantilever-based approach. (b) Experimental results for near-field thermal conductance vs gap size measured between a 100 μm diameter silica sphere and a glass slide (blue circles), doped Si surface (green squares), and Au surface (red triangles). The curves correspond to the theoretical results computed with the proximity approximation within fluctuational electrodynamics (FE). (a, b) Reprinted from ref 15. Copyright 2009 American Chemical Society. (c) Schematic illustration of the NFRHT measurement configuration. The emitter microdevice comprises a square mesa and a Pt heater/thermometer suspended on a thermally isolated island. The receiver is a macroscopically large (1 cm × 1 cm) plate. (d) Heat flux versus gap size. Measured data (red squares) are compared to the theoretical result (solid black line) obtained within FE. (c, d) Reprinted from ref 34. Copyright 2018 American Chemical Society. (e) Schematic of the experimental setup in which a scanning thermal microscopy probe is in close proximity to a heated substrate. (f) Measured near-field radiative conductance between a SiO_2-coated probe (310 K) and a SiO_2 substrate at 425 K. The red solid line shows the average conductance from 15 independent measurements, and the light-red band represents the standard deviation. The blue solid line shows the average of the computed radiative conductance for 15 different tips with stochastically chosen roughness profiles (root-mean-square roughness of ∼10 nm) and a tip diameter of 450 nm. The blue-shaded region represents the standard deviation of the calculated data. Reprinted with permission from ref 26. Copyright 2015 Springer Nature.

transfer. The statistical average of these currents vanishes (i.e., $\langle \mathbf{J} \rangle = 0$), but their correlations are given by the fluctuation–dissipation theorem:[110,111]

$$\langle J_i(\mathbf{r}, \omega) J_j^*(\mathbf{r}', \omega) \rangle = \frac{4}{\pi} \epsilon_0 \omega \, \mathrm{Im}\{\epsilon(\mathbf{r}, \omega)\} \Theta(\omega, T(\mathbf{r})) \delta(\mathbf{r} - \mathbf{r}') \delta_{ij} \quad (6)$$

where $\Theta(\omega, T(\mathbf{r})) = \hbar\omega/(\exp[\hbar\omega/k_B T(\mathbf{r})] - 1)$. To compute the radiative heat transferred from body 1 to body 2, we first have to solve the Maxwell equations with the appropriate boundary conditions set by the geometries of the bodies and assuming that the random currents occupy the whole body 1. Then, with the solution for the fields inside body 2, we must compute the statistical average of the Poynting vector: $\langle \mathbf{S}(\mathbf{r}, \omega) \rangle = \mathrm{Re}\langle \mathbf{E}(\mathbf{r}, \omega) \times \mathbf{H}(\mathbf{r}, \omega) \rangle/2$. Finally, we must integrate the results over frequency and the whole region of body 2. Of course, to evaluate the net RHT, we need to calculate in a similar way the heat transferred from body 2 to body 1, a task that is alleviated by detailed balance.

This generic problem can be quite challenging, and analytical solutions have been found in only a few cases with simple geometries such as two parallel plates[8] (see previous section), two spheres,[112] or a sphere in front of a plate.[113] In general, in order to solve this problem for complex geometries, one has to resort to numerical methods. In this respect, a lot of progress has been made in recent years, and standard numerical methods in electromagnetism have already been combined with FE to describe NFRHT between objects of arbitrary size and shape.[114] One of the most popular methods is the scattering matrix approach, which is specially suited to deal with layered planar structures,[8,115−118] including periodically patterned planar systems such as gratings or photonic crystals,[119] but can also be used to describe the RHT between arbitrary objects.[120−122] Other general-purpose approaches for modeling RHT between bodies of arbitrary shape are based on finite-difference time- and frequency-domain methods.[123−126] Probably the most efficient method for dealing with homogeneous finite objects of arbitrary shape is the so-called fluctuating surface current (FSC) method put forward by Rodriguez and co-workers,[127,128] which is based on the surface integral equation formulation of classical electromagnetism and has been combined with the powerful boundary element method (BEM) in the code SCUFF-EM.[129] All of these methods are meant to describe homogeneous systems with constant temperature profiles. To go beyond this, in recent years several numerical methods based on volume integral equations have been developed, such as the fluctuating volume current (FVC) approach,[130] which is the natural extension of the FSC method mentioned above, and the thermal version of the discrete dipole approximation (TDDA).[131−133] Both of these approaches are able to describe situations where the dielectric functions vary in space and the temperature has arbitrary profiles. They are well-suited to describe situations

DOI: 10.1021/acsphotonics.8b01031
ACS Photonics 2018, 5, 3896−3915

where the object sizes are on the order of or smaller than the relevant wavelengths, with the TDDA method having more problems handling situations in which there are large refractive index contrasts.

In spite of the remarkable progress made in recent years in the development of theoretical approaches to compute RHT (in both the near- and far-field regimes), there are still basic open problems. It continues to be very challenging and time-consuming to compute the RHT between microstructures of arbitrary shapes. This is particularly difficult, and often unmanageable, in the case of structures with complex combinations of materials and in the presence of nontrivial temperature profiles. On the other hand, most of the calculations based on FE are done within the local approximation, i.e., assuming that the dielectric function depends only on the frequency and not on the wave vector. Nonlocal effects may play a role in the extreme case of nanometer-sized gaps, and their impact still needs to be clarified.[108,134] Also, in that extreme near-field regime, thermal radiation may compete with other energy transfer mechanisms such as heat conduction (mediated by electrons or phonons).[135,136] In this sense, it would be nice to develop novel approaches to describe the contributions of different types of heat carriers on an equal footing.[137]

PROBING NFRHT

Although the NFRHT enhancement discussed above was predicted in 1971[8] and already hinted in several experiments in the late 1960s,[138−140] it was not until the late 2000s that this enhancement was unambiguously confirmed. Apart from the inherent difficulties of measuring any type of heat transfer, access to the near-field contribution requires exquisite control of the distance and alignment of macroscopic objects. Let us recall that, as shown in Figure 1c,e, nanoscale gaps are required to observe a sizable enhancement over the blackbody limit at room temperature. Moreover, the largest enhancements are predicted to occur between two parallel plates. However, this plate−plate configuration is one of the most difficult geometries to realize in practice because it is extremely complicated to achieve and maintain good parallelism between macroscopic plates at nanometer separations. Some of these problems can be partially alleviated by employing a sphere−plate configuration, and actually, this was the scheme used in some of the first experiments that clearly demonstrated the contribution of the near field to the RHT.[13−15,17,19,20,23,25] In Figure 3a,b we show an example of such a sphere−plate experiment based on a bimaterial cantilever approach. In this case, the RHT between a 100 μm diameter silica sphere and three different surfaces made of silica, Au, and doped Si was measured for gap sizes ranging from 10 μm down to around 30 nm. As shown in Figure 3b, the near-field conductance exhibits a clear enhancement as the gap is reduced, particularly in the case of the silica surface.

In the case of sphere−plate configurations, the NFRHT enhancements are rather modest because of the curvature of the spheres. To further increase this enhancement, in recent years different groups have developed novel techniques to explore the plate−plate configuration. Some of those experiments have been done using macroscopic (~cm × cm) planar surfaces,[12,16,30,33,139] while others have employed microscopic plates (50 μm × 50 μm).[24,28,29,34] The use of macroscopic planar surfaces is conceptually simple, but in practice it is more difficult to ensure the parallelism and to have pristine and smooth surfaces over such large areas. For this reason, the smallest gaps achieved with this strategy are on the order of several hundred nanometers.[33] On the other hand, the use of microdevices facilitates parallelization of the systems and characterization of the surfaces. With this approach, it has become possible to explore gaps as small as 30 nm,[34] as illustrated in Figure 3c,d. In this example, a microdevice comprising a Pt resistor, which is used both to heat up the emitter and to measure its temperature, was used to measure the NFRHT between two SiO_2 surfaces all the way down to 30 nm. For these tiny gaps, it was found that the heat conductance was about 1200 times larger than in the far-field regime and about 700 times larger than the blackbody limit.[34]

With these different techniques and configurations, it has become possible to measure the NFRHT between different types of materials, such as metals,[13,29] where the heat transfer is dominated by frustrated total internal reflection modes; polar dielectrics,[14,15,28,29,33,34] where the NFRHT is mediated by SPhPs; and doped semiconductors,[23,27] where infrared surface plasmon polaritons (SPPs) play a fundamental role. It has also been possible to explore more exotic materials like VO_2,[19] which undergoes a metal-to-insulator transition at 68 °C, and even graphene.[20] It is worth mentioning that it has also been possible to demonstrate that thin films of polar dielectrics exhibit NFRHT enhancements comparable to bulk samples.[25] Overall, these experiments have firmly established the validity of the theory of FE to describe the NFRHT for gaps larger than a few tens of nanometers. Moreover, the corresponding techniques have become sufficiently sophisticated to start exploring more complex NFRHT phenomena, like the ones that we shall discuss in the following sections.

The extreme near-field regime, for separations of <10 nm, has also been studied in recent years with the help of so-called scanning thermal microscopy (SThM) probes.[11,22,26,31,32] In this case, a scanning probe incorporating a thermocouple is used to measure the heat transfer between the probe and a substrate down to gaps of a few nanometers using SThM probes in AFM mode[26] and even down to a few angstroms using the probes in STM mode.[11,22,31,32] Using this latter mode, a group at the University of Oldenburg has systematically reported signals in the extreme near-field regime that completely defy the theory of FE.[11,22,32] Thus, for instance, in a recent work this group measured the heat transfer between a Au-coated tip and a Au surface at distances of 0.2−7 nm and found that the heat flux is 4 orders of magnitude larger than the values predicted by FE.[32] It has been suggested that this could be due to the contribution of an additional nonradiative mechanism operating in the crossover regime between radiation and conduction, although the reported signals are not compatible with standard models for the contributions of phonons and electrons. On the other hand, a group at the University of Michigan carried out a systematic study using SThM probes in AFM mode for gaps down to 2−3 nm.[26] The advantage of this approach is that the probes can be coated with almost any material, and thus, the radiative heat transfer between nonconductive materials can also be measured. In that work, the extreme NFRHT between polar dielectrics like SiO_2 and SiN and metals like Au was studied, and in all cases the results were found to be in excellent agreement with very detailed simulations performed within the local approximation of FE and no adjustable parameters.[26] Moreover, in order to shed new light on the striking results of the Oldenburg group, the Michigan team also conducted Au−Au experiments in

DOI: 10.1021/acsphotonics.8b01031
ACS Photonics 2018, 5, 3896−3915

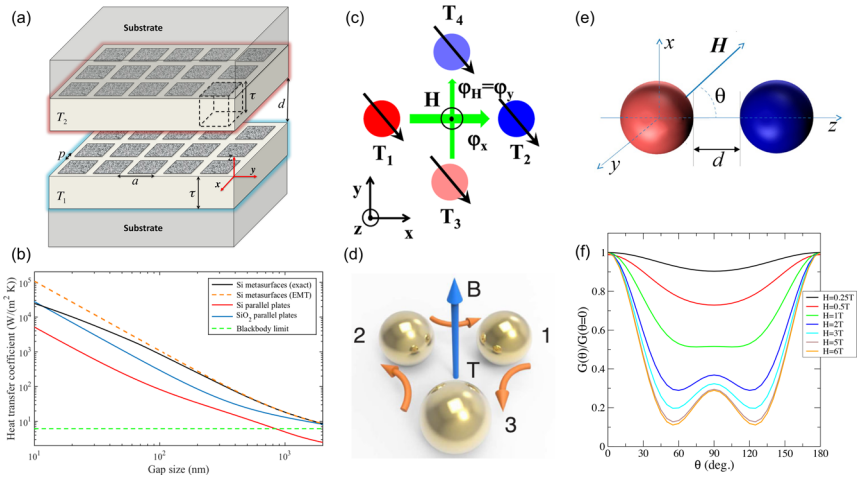

Figure 4. Tunability and active control of NFRHT. (a) Schematic of two doped Si metasurfaces made of 2D periodic arrays of square holes placed on semi-infinite planar substrates and held at temperatures T_1 and T_2. (b) Room-temperature heat transfer coefficient as a function of gap size for the doped Si metasurfaces in (a) with a = 50 nm and a filling factor of 0.9 (black line). For comparison, the plot also includes results for Si metasurfaces computed with effective medium theory (orange dashed line), SiO_2 parallel plates (blue line), and doped Si parallel plates (red line). The horizontal dashed line shows the blackbody limit. (a, b) Reprinted with permission from ref 179. Copyright 2017 American Physical Society. (c) Sketch of a four-terminal junction made with magneto-optical nanoparticles used to demonstrate the existence of a photon Hall effect under the action of an external magnetic field **H** when the left and right particles are held at two different temperatures. If a magnetic field is applied in the z direction, the particles become biaxial, breaking the system symmetry, and a temperature gradient is generated in the y direction, giving rise to a non-null Hall flux. Reprinted with permission from ref 186. Copyright 2016 American Physical Society. (d) System of three bodies consisting of spheres made of magneto-optical materials forming an equilateral triangle, with a magnetic field applied perpendicular to the plane of the triangle. This system exhibits a persistent directional heat current in thermal equilibrium. Reprinted with permission from ref 187. Copyright 2016 American Physical Society. (e) Schematic of a system with two identical magneto-optical particles of radius r held at different temperatures and separated by a gap d. A magnetic field **H** lying in the xz plane is applied in a direction forming an angle θ with the heat transport direction (z axis). (f) Room-temperature thermal conductance as a function of the angle θ between the magnetic field and the transport direction for two InSb particles of radius 250 nm, a gap of 500 nm, and different values of the magnetic field magnitude. The conductance is normalized by the conductance at $\theta = 0$. (e, f) Reprinted from ref 189. Copyright 2018 American Chemical Society.

STM mode.[31] They also found giant signals for gaps between 5 nm and a few angstroms. However, after the system was systematically cleaned, those signals decreased below the detection limit, as expected from FE calculations. Moreover, they showed that the presence of contamination can be detected by measuring the apparent tunneling barrier height from the tunneling current data. These results strongly suggest that the giant signals reported in the extreme near-field regime are indeed due to the presence of surface contaminants that provide additional paths for heat transfer via conduction. Let us also say that those giant signals are also not compatible with recent results on the heat conductance of gold atomic-sized contacts,[147,148] where the heat conductance is dominated by electron transport with a smaller contribution due to phonon conduction.[149] In any case, it would be highly desirable to report more experiments in this extreme near-field regime to further clarify this issue. More importantly, it would be crucial to improve the sensitivity of the SThM probes to be able to investigate the crossover between radiation and conduction both in metals and in dielectrics.

All of the experiments mentioned so far in this section aimed to measure the NFRHT, but they did not provide spectral information. As we showed above, the heat flux spectral distribution can drastically differ from Planck's distribution, and some of the potential applications of NFRHT are actually related to the possibility of conveniently tuning the spectral heat flux. Therefore, there is a great interest in experiments that can provide spectral information on the near-field thermal radiation. The first experiment with this purpose in mind was reported by De Wilde and co-workers back in 2006.[38] In that work, the authors made use of a thermal radiation scanning tunneling microscope (TRSTM) that enabled high-resolution imaging of surfaces by using the near-field thermal radiation as an intrinsic source of illumination. The basic idea was to bring a sharp W tip into close proximity (a few hundred nanometers) of a sample in order to scatter the evanescent electromagnetic field into the far field, where it is detected and analyzed with a spectrometer. This experiment showed a limited spectral resolution, but it demonstrated excellent imaging capabilities. In recent years, several groups have perfected this idea with the hope to have access, in particular, to the local density of states (LDOS) of electromagnetic modes close to a sample of interest.[40,141−145] In spite of the remarkable advances in this topic, it is still unclear what is the exact relation between the detected far-field signals and the LDOS and how invasive the tips actually are.[146] In this sense, more work needs to be done, both theoretically and experimentally, in order to elucidate those issues. Moreover, an important breakthrough would be the development of experimental setups to simultaneously measure the spectral properties of the far-field signals and the NFRHT between the tip and the sample. The correlation between those two types of signals could provide a very valuable novel insight into near-field thermal radiation.

TUNABILITY AND ACTIVE CONTROL OF NFRHT

Since the confirmation of the basic prediction of the NFRHT enhancement, there has been a huge amount of theoretical work suggesting new ideas and strategies to further enhance the NFRHT and tune its spectral properties. A strategy has been based on the use of layered planar structures, including

DOI: 10.1021/acsphotonics.8b01031
ACS Photonics 2018, 5, 3896−3915

thin films, with the goal, in particular, to make better use of surface electromagnetic modes.[150−157] Another idea that has been thoroughly studied is the use of metamaterials with complex optical properties. In particular, hyperbolic metamaterials have received a lot of attention because they have been predicted to behave as broad-band super-Planckian thermal emitters.[158−160] These metamaterials are a special class of highly anisotropic media that have hyperbolic dispersion. To be precise, they are uniaxial materials for which one of the principal components of either the permittivity tensor or the permeability tensor is opposite in sign to the other two principal components. These media have been mainly realized by means of hybrid metal−dielectric superlattices and metallic nanowires embedded in a dielectric host.[161] What makes these metamaterials so special for NFRHT is the fact that they can support electromagnetic modes that are evanescent in a vacuum gap but propagate inside the material. This leads to a broad-band enhancement of the transmission efficiency of the evanescent modes.[159] This special property has motivated a lot of theoretical work on the use of hyperbolic metamaterials for NFRHT.[162−170] This work has shown that actually these metamaterials do not outperform thin-film structures exhibiting surface phonon polaritons, but the long penetration depth of the hyperbolic modes can be advantageous for applications like near-field thermophotovoltaics.

Inspired by nanophotonic concepts, different authors have studied theoretically the NFRHT between periodically patterned systems in both one and two dimensions with the hope of tuning the spectral heat transfer and enhancing the NFRHT. Thus, for instance, several groups have reported calculations of the NFRHT between periodic metallic nanostructures in both one[171−174] and two dimensions.[175] The idea in this case is to create via nanostructuration new surface modes, called spoof plasmons,[176] whose frequencies can be adjusted by tuning the length scales of the periodic systems such that they lie in the infrared region and thus can contribute to the heat transfer at room temperature. These calculations have shown a good degree of tunability and the possibility to enhance NFRHT over the corresponding material without nanostructuration. However, the reported NFRHT in these metallic structures is still much smaller than in the simple case of parallel plates made of polar dielectrics. There have also been theoretical studies of the NFRHT between photonic crystals and periodic metamaterials made of dielectrics[123,177,178] that show how the radiative properties can be enhanced with respect to the bulk counterpart. However, the resulting NFRHTs are again much smaller than those of planar polar dielectrics. Building upon these ideas, it has recently been predicted that metasurfaces can provide a viable strategy to tune and enhance the NFRHT between extended structures.[179] In particular, it has been shown that Si-based metasurfaces featuring two-dimensional periodic arrays of holes (Figure 4a) can exhibit a room-temperature near-field radiative heat conductance much larger than that of any unstructured material to date (Figure 4b). This enhancement relies on the possibility to largely tune the properties of the surface plasmon polaritons that dominate the NFRHT in these structures. In particular, the nanostructuration of these metasurfaces produced broad-band surface modes that are occupied at room temperature, which actually constitutes one of the main strategies that is being pursued to enhance NFRHT. Let us also mention that very recently Jin et al.[180] made use of inverse design to show that the RHT between generalized two-dimensional gratings made of lossy metals can lead to a huge frequency-selective enhancement of NFRHT.

Presently, one of key challenges in this field is to actively control NFRHT. In this respect, several interesting ideas have been put forward in recent years. An appealing idea is based on the use of phase-transition materials,[181,182] where a change of phase, induced by applying an electric field or changing the temperature, results in a change in the radiative heat transfer (more about these materials is presented in the following section). Another possibility that has been theoretically investigated is the use of chiral materials with magnetoelectric coupling in which the NFRHT can be tuned by ultrafast optical pulses.[183] It has also been predicted that NFRHT can be actively controlled by using ferroelectric materials under an external electric field,[184] although the predicted changes are rather small (<17%). More recently, it has also been proposed that the heat flux in systems involving semiconductors can be controlled by regulating the chemical potential of photons by means of an external bias.[61] This idea could be the basis of different thermal management devices and will be discussed in the next section. On the other hand, magneto-optical (MO) objects have been put forward as a promising avenue to control NFRHT with an external magnetic field.[185] In particular, it has been shown that the NFRHT between two parallel plates made of doped semiconductors can be strongly affected by the application of a static magnetic field, and relative changes of up to 700% can be induced with fields of a few teslas.[185] Furthermore, it has recently been predicted that the lack of reciprocity in these MO systems may lead to a number of novel fundamental thermomagnetic effects such as a near-field thermal Hall effect[186] (Figure 4c) and the existence of a persistent heat current[187] (Figure 4d). Moreover, it has been shown that these MO systems under a static magnetic field can exhibit the near-field thermal analogues of the key effects in the field of spintronics, such as giant thermal magnetoresistance[188] or anisotropic thermal magnetoresistance[189] (this effect is illustrated in Figure 4e,f).

The obvious challenge for the near future is the experimental verification of all these attractive ideas, which to date have only been addressed theoretically. As mentioned above, the recent advances in the experimental techniques to measure NFRHT should soon make possible proofs of concept for many of the ideas discussed in this section.

NEAR-FIELD THERMAL MANAGEMENT

The next step beyond the active control of NFRHT is to make use of it in functional devices. In this respect, there has been a lot of work in particular to propose and realize near-field thermal analogues of the key building blocks in electronics: diodes, transistors, switches, memory elements, etc. The diode is the device that has attracted by far the most attention. It has been shown that thermal rectification can be achieved by using asymmetric systems (involving dissimilar materials) with temperature-dependent optical properties. Thus, for instance, there are a number of theoretical proposals involving different combinations of materials, including SiC structures,[43] doped Si films,[190] a dielectric coating,[191] and Si and a different material.[192] Special attention has been paid to the use of phase-transition materials.[193−199] A prototypical example is vanadium dioxide (VO_2), which undergoes a phase transition from and insulator below 68 °C to a metal above that temperature. This phase transition results in a drastic change in the infrared optical properties, which is manifested in the

DOI: 10.1021/acsphotonics.8b01031
ACS Photonics 2018, 5, 3896−3915

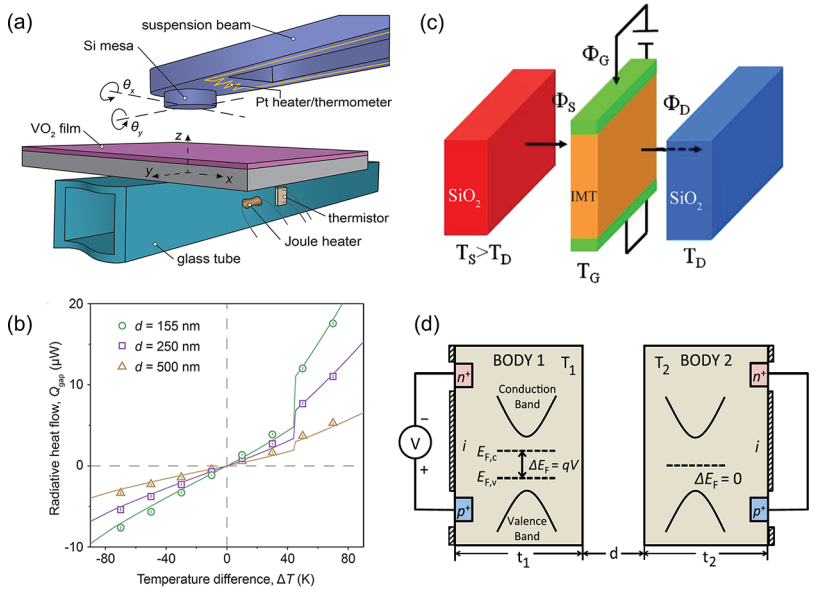

Figure 5. Near-field thermal management. (a) Schematic illustration of a radiative thermal diode consisting of a cantilever with an embedded Pt heater/thermometer and a VO_2 sample. (b) Total radiative heat flow as a function of the temperature difference $\Delta T = T_{VO_2} - T_{Si}$ for three selected values of the vacuum gap size d in the setup shown in (a). The symbols correspond to the measured values, while the solid lines correspond to the modeling results with the phase transition occurring at 68 °C. (a, b) Reprinted from ref 45. Copyright 2018 American Chemical Society. (c) Radiative thermal transistor in which a layer of an insulator−metal transition (IMT) material (the gate) is placed at subwavelength distances from two thermal reservoirs (the source and the drain). The temperatures of the reservoirs are fixed, while the temperature T_G of the gate can be modulated around its steady-state temperature. Reprinted with permission from ref 44. Copyright 2014 American Physical Society. (d) Schematic of a solid-state cooling device that consists of two intrinsic semiconductors that are brought into close proximity with a vacuum gap separation d. To control the chemical potential of each semiconductor, the back side of each intrinsic semiconductor region contains a junction with a small heavily doped p or n region, which then connects to external contacts. An external forward bias V is applied to body 1, while body 2 is shorted. Reprinted with permission from ref 61. Copyright 2015 American Physical Society.

corresponding NFRHT in systems involving this material as the temperature is varied across the transition temperature.[181,182,200] Actually, several experiments have already demonstrated rectification between VO_2 and SiO_2 in the far-field regime.[19,200,201] The first observation of rectification in the near-field regime was reported very recently by Fiorino et al.[45] In that work, the authors explored the NFRHT between a Si microdevice and a macroscopic VO_2 film (Figure 5a). They observed clear rectifying behavior that increased at nanoscale separations (see Figure 5b), with a maximum rectification ratio exceeding 50% at ∼140 nm gaps and a temperature difference of 70 K. This high rectification ratio was attributed to the broad-band enhancement of heat transfer between metallic VO_2 and doped Si surfaces, compared with the narrower-band exchange that occurs when VO_2 is in its insulating state.

Building upon the idea of thermal diodes based on a phase-transition material, Ben-Abdallah and Biehs[44] proposed the realization of a near-field thermal transistor. The proposed transistor, which is schematically represented in Figure 5c, consists of a three-body system (two diodes in series) in which a layer of a metal-to-insulator transition material (the gate) is placed at subwavelength distances from two thermal reservoirs (the source and the drain). The temperatures of the reservoirs are fixed, while the temperature of the gate can be modulated around its steady-state temperature. Those authors showed that changing the gate temperature around its critical value allows the heat flux exchanged between the hot body (source) and the cold body (drain) to be reversibly switched, amplified, and modulated by a tiny action on the gate. On the other hand, the same authors extended these ideas to propose other key elements such as a thermal memory,[202] and they have also shown that thermal logic gates can be realized by exploiting the near-field radiative interaction in N-body systems with phase-transition materials.[203] These proposals are nicely reviewed in ref 204.

A very interesting idea for the topic of near-field thermal management has recently been put forward by Fan's group. In most of the works on NFRHT discussed above, it is assumed that the chemical potential of the involved objects is zero. However, photons can have a chemical potential when they are in quasi-equilibrium with a semiconductor under an external bias.[205] In particular, when a semiconductor p−n junction is under an external bias, the expectation value of the photon energy per mode above the band gap satisfies the Bose−Einstein distribution:

$$\Theta(\omega, T, V) = \frac{\hbar\omega}{e^{(\hbar\omega - qV)/k_B T} - 1} \tag{7}$$

where q is the magnitude of the electron charge, V is the external bias, and T is the temperature of the semiconductor. Thus, in the presence of a bias (positive or negative), the photon emission of the p−n junction is altered compared with the same system at $V = 0$, and therefore, one can use this idea to control the NFRHT between two bodies. On the basis of this idea, Fan and co-workers proposed several strategies to use NFRHT for solid-state cooling.[61,62] One of them is schematically represented in Figure 5d. In this case, two intrinsic semiconductors are brought into close proximity and held at different temperatures. To control the chemical potentials of the individual semiconductors, they contain a p−n junction in the back side. In this case, by applying a positive bias to the cold body (semiconductor 1) while the hot body (semi-

DOI: 10.1021/acsphotonics.8b01031
ACS Photonics 2018, 5, 3896−3915

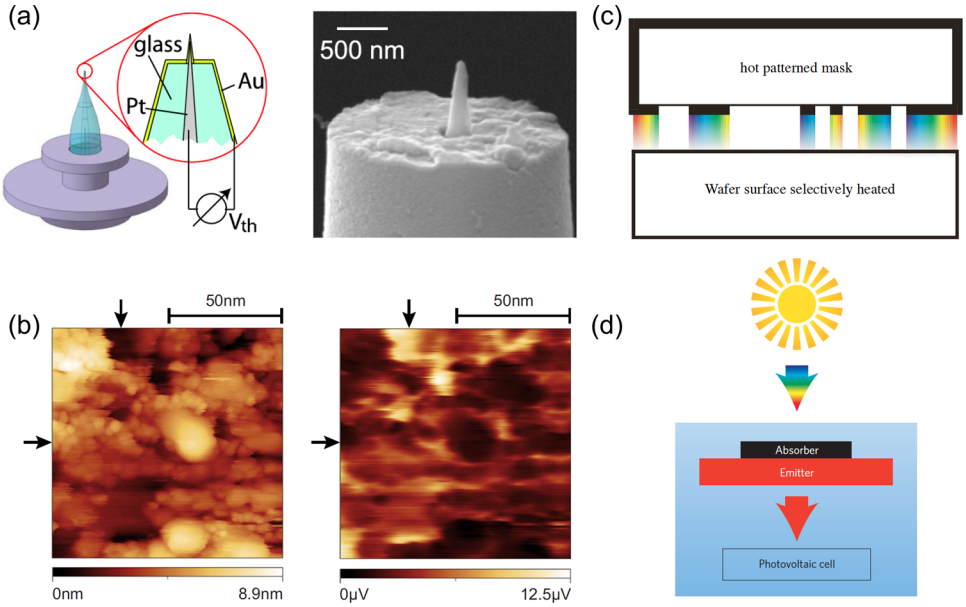

Figure 6. NFRHT potential applications. (a) Schematic drawing of a scanning thermal microscopy (SThM) tip in its holder, displaying the glass capillary, the platinum wire, and the gold coating that form the thermocouple.[39] On the right-hand side one can see a scanning electron microscopy image of a typical SThM tip. The platinum wire protrudes from the center of the glass mantle. Both are covered by a gold film. (b) (left) STM topography of a gold surface on mica taken with an SThM tip and (right) corresponding spatial distribution of the local thermovoltage measured by the thermocouple. The temperature of the sample is 110 K, and that of the probe is 293 K. (a, b) Reprinted from ref 39. Copyright American Institute of Physics. (c) Working principle of near-field thermal lithography.[37] A mask is patterned using two materials, one that is a poor emitter of evanescent waves at the ambient temperature and another that is a good emitter. A wafer placed close to the mask will be selectively heated beneath the good emitter, an effect that may possibly be exploited to selectively etch the wafer to much higher resolution than possible with conventional methods. (d) Working principle of a solar thermophotovoltaic (STPV) cell. A standard photovoltaic cell is directly exposed to sunlight. In an STPV cell, an intermediate material is placed between the sun and the photovoltaic cell. The intermediate material absorbs the sunlight, heats up, and generates thermal radiation that is emitted toward the photovoltaic cell. Reprinted with permission from ref 211. Copyright 2014 Springer Nature.

conductor 2) is shorted ($V = 0$), one can achieve a net heat flow from the cold object to the hot object.[61] A related idea is to apply a negative bias to a p−n junction, which according to eq 7 results in the emission of fewer photons. This suppression of the thermal radiation from a semiconductor p−n junction by applying a negative bias is known as negative luminescence and has several applications. In the context of solid-state cooling, negative luminescence can be used to extract heat from a cold body to a hot one. The idea is to apply a negative bias to a semiconductor featuring a p−n junction and to bring it into close proximity of a colder object. In this case, one can show again that a net heat flow from the cold object to the hot object is possible. This idea was actually explored long ago in the far-field regime[206] and now has been shown to be much more efficient in the near-field regime.[62,207,208]

OTHER POTENTIAL NFRHT APPLICATIONS: THERMOPHOTOVOLTAICS

We have already mentioned a number of potential applications of NFRHT, but these are by no means the only ones. Thus, for instance, the techniques mentioned above for NFRHT measurements based on scanning thermal microscopy probes can be used for imaging.[22,38,39] This is illustrated in Figure 6a,b, which shows how a SThM probe at room temperature was operated in constant-current STM mode to scan a cooled (100 K) Au substrate while simultaneously recording the tip thermovoltage.[39] The comparison between the STM topography and the thermovoltage images clearly shows that this thermal microscopy technique does indeed give information about the topography of the surface. It remains to be seen whether this approach can become a standard imaging technique that could somehow complement STM or AFM techniques to scan conductive and nonconductive surfaces.

Other potential applications include Pendry's proposal to use near-field radiation for high-resolution thermal lithography[37] (Figure 6c). It has also been suggested that the understanding of RHT, especially in the extreme near-field regime, could be important for optimizing the performance of heat-assisted magnetic recording technologies.[35,36]

The most promising and important NFRHT applications are those related to energy conversion and, in particular, thermophotovoltaics (TPVs). It is well-known that the efficiency of a single-junction solar cell is subject to the so-called Shockley−Queisser limit and cannot exceed ∼41%.[209] This limit arises from the mismatch between the broad-band solar radiation spectrum and the electronic band structure of the semiconductors used in solar cells. The point is that photons with energies below the semiconductor band gap cannot be used to generate electricity, while part of the energy of the photons with energies above the gap is lost in the form of heat because photon-generated carriers must first relax to the semiconductor band edges. In order to overcome the Shockley−Queisser limit, in 1979 Swanson[210] put forward the concept of solar thermophotovoltaic (STPV) systems, which is illustrated in Figure 6d. The idea is to place an intermediate element between the sunlight and the solar cell. This intermediate element includes an absorber that can absorb the entire solar spectrum and an emitter that can generate narrow-band thermal radiation with frequencies close to the band gap of the solar cell. It has been shown that a strategy like this could help boost the efficiency of solar cells and clearly

DOI: 10.1021/acsphotonics.8b01031
ACS Photonics 2018, 5, 3896−3915

overcome the Shockley−Queisser limit[212] (estimates suggest that the efficiency could reach up to ∼85% for nonreciprocal cells). On the other hand, this basic idea can also be used in applications such as recovery of low-grade waste heat, where a hot object can be used as the hot emitter in a TPV cell instead of the sun. However, the efficiency of these TPV devices is usually limited by the low temperatures available in waste heat recovery applications (<1000 K).

The TPV cell concept was introduced having in mind conventional far-field RHT between a hot emitter and a PV cell (see the next section), but it is obvious that NFRHT could have a great impact in TPV technology because of the enhanced thermal radiation and the possibility to tune the radiation spectrum. The enhanced heat fluxes in the near field would lead to an increase in the power output of the cells, while tuning of the spectral radiation may help to reach the Carnot limit for the efficiency of TPV cells, where the only limitation is then set by the temperature of the hot emitter (let us stress that, as shown in the next section, the spectral radiation can also be largely tuned in the far-field regime). In recent years, there has been a huge amount of theoretical work exploring different ideas on how NFRHT can be used to boost the efficiency of TPV cells for waste heat recovery applications.[46−58] These works have clearly illustrated the great potential of NFRHT in this energy conversion application. From the experimental side, most of the efforts to date have focused on far-field strategies (see the next section), but there have already been some experimental reports exploring the impact of NFRHT.[213,214] A very convincing proof of concept of the potential of near-field TPV cells was reported very recently by Fiorino et al.,[59] who employed a microdevice made of Si as a hot emitter and InAsSb PV cells with low band gaps of 0.345 and 0.303 eV. The microdevice allowed them to bring the hot emitter within submicron distances of the PV cell and to create and maintain large temperature differences while keeping the emitter and the receiver parallel with the help of a nanopositioner. They characterized the performance of these near-field TPV devices using temperatures between 525 and 655 K for the hot emitter and exploring gap sizes from 20 μm all the way down to a few tens of nanometers. They demonstrated that such near-field devices can generate 40 times more power with 60 nm gaps than at large separations (far-field regime). They attributed this enhanced performance to the contribution of photon tunneling originating from frustrated total internal reflection modes. The challenge now is to scale-up this technique to explore large-area devices and to optimize it to be able to compete with thermoelectric approaches for waste heat recovery.

NANOPHOTONIC CONTROL OF THERMAL RADIATION AND ENERGY APPLICATIONS

We now turn to the far-field regime and in this section focus on control of the far-field thermal radiation of an emitter and its energy applications. Traditionally, the far-field radiation was believed to be incoherent, broad-band, almost isotropic, and unpolarized. Moreover, thermal emission was supposed to be subject to two fundamental constraints. The first one is Planck's law, which sets a limit on the spectral density of the thermal radiation per unit area. The second one is Kirchhoff's law, which in simple terms tells us that the emissivity of an emitter must be equal to its absorptivity (for every frequency, angle, and polarization). However, in the last 20 years, through the use of the concepts and techniques of nanophotonics, all of these conventional ideas about thermal emission have been challenged, which in turn has paved the way for the development of novel thermal applications. In what follows, we shall briefly summarize the recent progress on this topic.

In most cases Kirchhoff's law actually applies (see below for exceptions), and thus, it can be used as a starting point to compute the emissivity of an object and therefore its thermal emission. The calculation of the absorptivity can be done using standard theoretical methods in photonics, and many groups have put forward different strategies to control the thermal emission. The basic idea is to use structures with feature sizes comparable to the relevant thermal wavelengths to control thermal emission in the same way that nanophotonic systems (with characteristic dimensions compared with the wavelength of light) are used to control light. Following this idea, it has been shown both theoretically and experimentally that one can control the spectral properties of the thermal emission (i.e., its frequency dependence), which is of special relevance for energy applications. In particular, a wide variety of resonant systems have been employed to give rise to narrow-band thermal emission. These include photonic crystals,[65,66,215−217] arrays of metallic antennas,[64,67] Fabry−Perot cavities,[218−221] and metamaterials,[222,223] just to mention a few. Similarly, nanophotonic approaches have also been employed to demonstrate control of the polarization of the thermal radiation[42,68−70] and the possibility of tuning its angular dependence.[42,71−77]

There has also been quite a bit of work exploring the limits of the two fundamental constraints described above. In the case of extended (or macroscopic) structures, the absorptivity is smaller than 1, and therefore, the emissivity must also be smaller than 1. Thus, a thermal emitter cannot emit more than a corresponding blackbody with the same area, whose spectral density of the total emission power is given by Planck's distribution,

$$I_{\mathrm{BB}}(\omega, T) = \frac{\omega^2}{4\pi^3 c^2} \frac{\hbar\omega}{\exp(\hbar\omega/k_{\mathrm{B}}T) - 1} \tag{8}$$

which gives us the total power emitted per unit frequency and emitter area. This formula suggests that a way to enhance the thermal emission is to place an emitter in a transparent dielectric medium with a refractive index n. In this case, in eq 8 the speed of light c must be replaced by c/n, and thus, the total emission can be increased by a factor n^2. This strategy has been termed thermal extraction, and it has been successfully explored in several works,[224,225] although it should be noted that this does not mean that thermal emission is greater than that of a blackbody of the same area in the same environment. With respect to Kirchhoff's law, it has been understood that this is not a fundamental constraint set by the second law of thermodynamics but rather arises from reciprocity. Therefore, there is a chance to violate this law in the case of nonreciprocal objects, i.e., in objects whose permittivity tensor is non-symmetric, such as in magneto-optical systems. Still, it has been shown that the thermal emission of a single nonreciprocal object fulfills Kirchhoff's law.[133] However, Zhu and Fan[100] demonstrated that when a nonreciprocal emitter interacts with two thermal baths (assumed to be blackbodies), one can actually violate this law, which could be of fundamental importance in thermal radiation harvesting. This discovery has motivated more theoretical work on the validity of Kirchhoff's law.[226,227]

DOI: 10.1021/acsphotonics.8b01031
ACS Photonics 2018, 5, 3896−3915

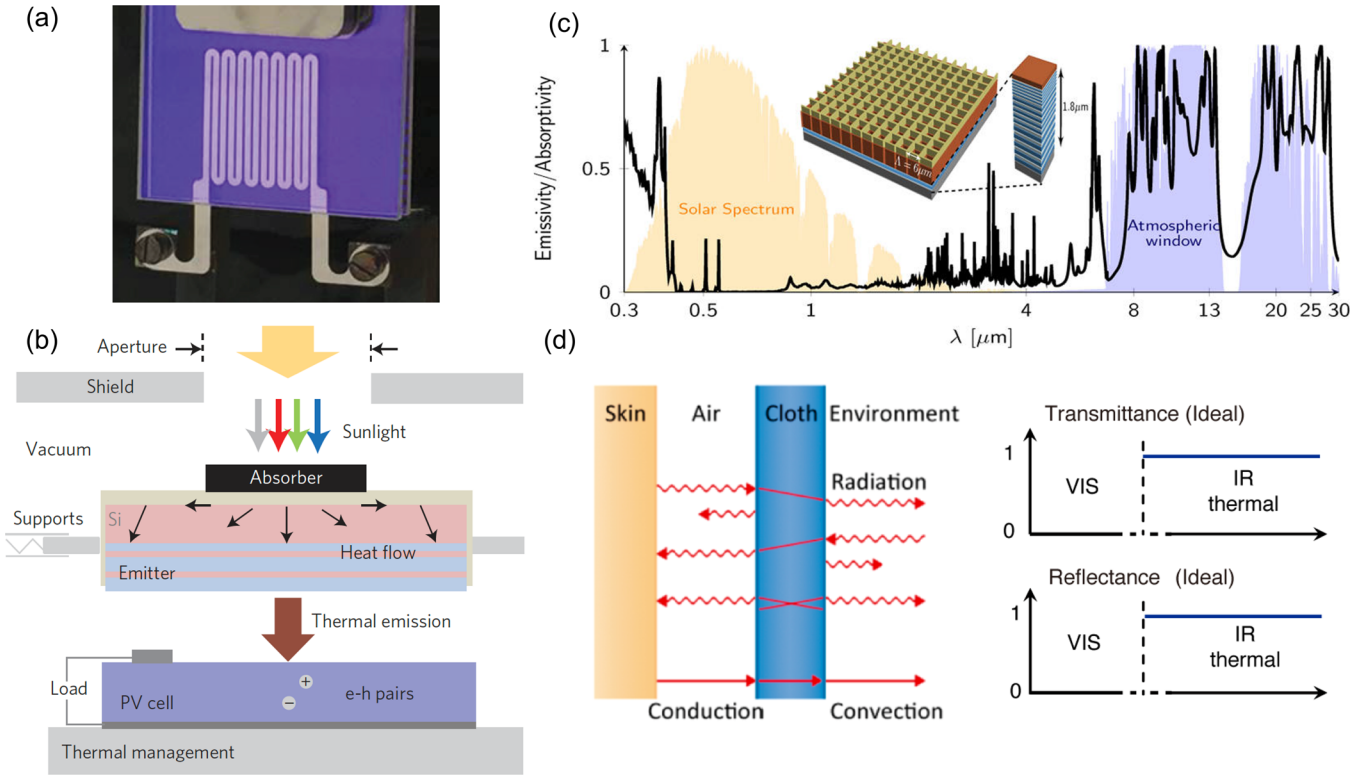

Figure 7. Nanophotonic control of thermal radiation for energy applications. (a) Incandescent light source: a tungsten emitter and surrounding interference stacks on a fused silica substrate. Reprinted by permission from ref 228. Copyright 2016 Springer Nature. (b) Experimental realization of a solar thermophotovoltaic system consisting of a broad-band absorber, a narrow-band emitter, and a InGaAsSb cell. Reprinted by permission from ref 98. Copyright 2016 Springer Nature. (c) Optimized daytime radiative cooler design consisting of two thermally emitting photonic crystal layers composed of SiC and quartz, below which lies a broad-band solar reflector. The graph shows the corresponding emissivity of the cooler at normal incidence (black) with the scaled AM1.5 solar spectrum (yellow) and atmospheric transmittance (blue) plotted for reference. The structure has minimal absorption throughout the solar spectrum and very strongly selective emission in the atmospheric transparency window, as is desirable and necessary for a high-performance daytime radiative cooler. Reprinted from ref 78. Copyright 2013 American Chemical Society. (d) Nanophotonic thermal textile for personal thermal management. (left) Schematic of heat dissipation pathways from a clothed human body to the ambient environment. Thermal radiation contributes to a significant part of total heat dissipation, in addition to heat conduction and heat convection. Reprinted from ref 86. Copyright 2015 American Chemical Society. (right) Ideal spectrum of the thermal textile for (top) cooling and (bottom) heating purposes.

The progress in the understanding of the control of thermal emission has led in recent years to a number of interesting energy applications. For instance, it has been demonstrated that the thermal emission of an incandescent tungsten filament (3000 K) can be modified by surrounding it with a cold-side nanophotonic interference system that is optimized to reflect infrared light and transmit visible light for a wide range of angles[228] (Figure 7a). In particular, it was shown that this system can reach luminous efficiencies of 40%, surpassing existing lighting technologies. Moreover, this strategy enables tailoring of the emission spectrum of high-temperature sources, which may find applications in thermophotovoltaics.

The concept of STPV cells, and TPV cells in general, as discussed in the previous section, actually arose in the context of far-field radiative heat transfer. In recent years, there has been a great amount of work concerning the use of nanophotonic strategies to design absorbers/emitters to increase the efficiency of TPV cells. In particular, important progress has been made in the experimental demonstration of STPV cells. For instance, Lenert et al.[98] reported promising experiments in which the absorber was made of vertically aligned multiwalled carbon nanotubes (Figure 7b). In those experiments, the emitter was made of one-dimensional Si/SiO_2 photonic crystals, and the thicknesses of different layers were chosen to provide a cutoff in the thermal emission right at the band gap of the InGaAsSb PV cell, strongly suppressing sub-band-gap thermal radiation. This system was shown to have a solar-to-electricity efficiency of 3.2%. In a subsequent experiment, Bierman et al.[99] improved the efficiency to 6.8% through suppression of 80% of the unconvertible photons by pairing a 1D photonic crystal selective emitter with a tandem plasma-interference optical filter.

In recent years it has been demonstrated that it is possible to cool down a system simply by exposing it to sunlight without any electricity input.[78,79] This counterintuitive possibility, known as passive radiative cooling, is based on the idea that the earth's atmosphere has a transparency window for electromagnetic radiation between 8 and 13 μm that coincides with the peak thermal radiation wavelengths at typical ambient temperatures. By exploiting this window, one can cool a body on the earth's surface by radiating its heat away into the cold out space. While nighttime radiative cooling has been widely studied in the past, only very recently has it been possible to demonstrate this phenomenon during daytime, which is obviously when the demand for cooling is highest. A first theoretical proposal of daytime radiative cooling was put forward by Rephaeli et al.[78] In this case, the cooler consists of two thermally emitting photonic crystal layers composed of

DOI: 10.1021/acsphotonics.8b01031
ACS Photonics 2018, 5, 3896−3915

SiC and quartz, below which lies a broad-band solar reflector (Figure 7c). Subsequently, the same group designed and fabricated a multilayer photonic structure consisting of seven dielectric layers deposited on top of a silver mirror.[79] This design, when placed in a rooftop measurement setup, was shown to reach a temperature that is 5 °C below the ambient air temperature in spite of having sunlight at about 900 W/m^2 directly impinging upon it. After this proof-of-concept demonstration, there has been intense research activity with the goal of further optimizing this daytime radiative cooling.[80−85] Let us also say that similar concepts have been applied in recent years to the cooling of solar cells.[95−97]

Another interesting application of nanophotonic control of thermal radiation is that of thermal textiles for personal thermal management (Figure 7d).[86−94] In this case, the idea is to provide heating or cooling to a human body and its local environment. The human skin has a very high emissivity (~0.98%) and thermal radiation constitutes about half of the total body heat loss[86]. In the design of thermal textiles, the guiding principle is to have infrared transparent materials to fully dissipate human body radiation for cooling purposes, while one needs infrared reflective materials for heating purposes (Figure 7d). For both applications, the textiles need to be opaque in the visible range. To tune the spectral properties, different strategies have been developed to introduce suitable nanostructures into textiles.[86−94]

To conclude this section, let us also say that all of the strategies discussed in previous sections in relation to near-field thermal management, such as negative luminescence, have their counterparts in the far-field regime.

SMALL OBJECTS: FAR-FIELD SUPER-PLANCKIAN RADIATIVE HEAT TRANSFER

As mentioned in the previous section, the thermal emission of a macroscopic object cannot overcome the Planckian limit.[101] However, in the case of small objects, with some of their dimensions being smaller than λ_{th}, the actual emissivity (equal to the absorptivity) is the corresponding absorption efficiency, i.e., the absorption cross section divided by the geometrical one. It is well-known that the absorption efficiency of small objects can be larger than 1,[102] and therefore, nothing prevents the thermal emission of a subwavelength object from being super-Planckian (i.e., larger than that of a blackbody with the same geometrical area). However, this is extremely difficult to achieve in practice. In fact, only a modest super-Planckian thermal emission has been predicted in rather academic situations,[103,104] and it has never been observed. There have been experiments exploring the thermal radiation of subwavelength objects (see, e.g., ref 229), and these experiments have revealed the failure of Planck's law, but no super-Planckian emission has ever been reported. In the case of heat transfer, until very recently there were no theoretical proposals, and it had also never been observed.

Recently, Fernández-Hurtado et al.[106] showed theoretically that the far-field RHT between objects with dimensions smaller than λ_{th} can overcome the Planckian limit by orders of magnitude. To reach this conclusion, they were guided by a relation between the far-field RHT and the directional absorption efficiency of the objects involved. In the simple case of two identical spheres, this relation tells us that the radiative power exchanged by the spheres at temperatures T_1 and T_2 and separated by a distance much larger than both λ_{th} and their radii is given by[106]

$$P = \pi A F_{12} \int_0^\infty Q^2(\omega)[I_{BB}(\omega, T_1) - I_{BB}(\omega, T_2)]\, d\omega \quad (9)$$

where A is the area of the spheres, F_{12} is a geometrical view factor,[1] $I_{BB}(\omega, T)$ is the Planck distribution function (see eq 8), and $Q(\omega)$ is the frequency-dependent absorption efficiency of the spheres, which in this case is independent of direction and polarization. As stated above, this efficiency adopts the role of an effective emissivity. For blackbodies, $Q(\omega) = 1$ for all frequencies, and eq 9 reduces to the Stefan−Boltzmann law. Now, since (as stated above) $Q(\omega)$ can be larger than unity, eq 9 suggests that super-Planckian far-field RHT might be possible if we find the right combination of materials and object shapes such that there is an efficient broad-band absorption close to the maximum of Planck's distribution at a given temperature.

As shown by Fernández-Hurtado et al.,[106] this is easier said than done, and although simple geometrical objects may exhibit an absorption efficiency larger than 1 for certain frequencies (due, e.g., to the existence of Mie resonances), this is not enough to exhibit a super-Planckian far-field RHT. However, those authors demonstrated that this is possible in the case of highly anisotropic objects with highly directional emission properties. In particular, they illustrated this phenomenon in the case of suspended pads made of polar dielectrics like SiN or SiO_2 (Figure 8a). These structures are widely used to measure the thermal transport through nanowires and low-dimensional systems.[230−235] These suspended pads are made of SiN and normally have lateral dimensions on the order of tens of micrometers, while their thickness is usually below 1 μm (i.e., much smaller than λ_{th} at room temperature). As displayed in Figure 8b, Fernández-

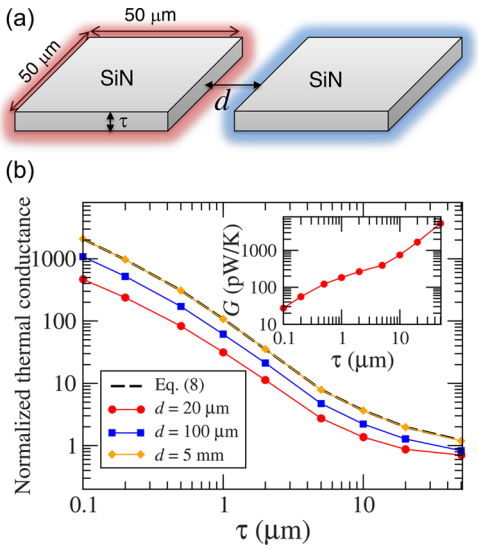

Figure 8. Super-Planckian far-field radiative heat transfer in SiN suspended pads. (a) SiN pads with lateral dimensions of 50 μm × 50 μm and thickness τ separated by a gap d. (b) Computed room-temperature radiative heat conductance, normalized by the blackbody results, for the system in (a) as a function of τ. The solid lines are the exact calculations for three gaps in the far-field regime (see the legend), and the black dashed line is the result obtained with a semianalytical approach valid in the extreme far-field regime. The inset shows the results for d = 20 μm without normalization. Reprinted with permission from ref 106. Copyright 2018 American Physical Society.

DOI: 10.1021/acsphotonics.8b01031
ACS Photonics 2018, 5, 3896−3915

Hurtado et al.[106] showed that as the thickness of these SiN pads decreases below λ_{th}, the thermal conductance becomes much larger than that of blackbodies of the same dimensions, in spite of the fact that two of the dimensions are still macroscopic. They attributed this extraordinary far-field RHT to the fact that these SiN pads behave as lossy dielectric waveguides that absorb the radiation very efficiently in the direction of the line that joins the two pads. The challenge now is to experimentally confirm these predictions, something that should be possible with the existing suspended-pad technology.[230−235] In fact, while this Perspective was in the review process, we became aware of the publication of work in which the far-field RHT between SiN suspended pads was measured and the fundamental findings of Fernández-Hurtado et al.[106] were verified.[236] In that work, the authors employed SiN pads with lateral dimensions of 60 μm × 80 μm and varying thickness (ranging from 270 nm to 11.4 μm). They reported conductance enhancements over the blackbody limit of around 2 orders of magnitude for the thinnest devices (270 nm) and showed that this enhancement persists for a wide range of temperatures (100−300 K). Moreover, in agreement with the results in Figure 8b, they showed that the enhancement over the blackbody result increases as the gap increases, and it is still visible at macroscopic distances on the order of 1 mm (see ref 236 for details).

To conclude this section, let us say that the violation of Planck's limit in the far-field regime was also studied by the same authors in the extreme case of two coplanar 2D materials (graphene and single-layer black phosphorus), i.e., materials with a one-atom-thick geometrical cross section.[107] In particular, it has been shown that the far-field RHT transfer between two coplanar graphene sheets can overcome the Planckian limit by more than 7 orders of magnitude. All of these results show the dramatic failure of the classical constraints for thermal radiation when we deal with micro- and nanodevices.

OUTLOOK

The field of radiative heat transfer has advanced much more in the last 10−15 years than in the previous 100 years. The progress in experimental techniques has finally enabled NFRHT to be probed in an almost routine way, and an avalanche of theoretical papers have put forward a great number of ideas related to novel thermal effects and their potential technological applications in both the near- and far-field regimes. However, there are still many open problems and basic challenges in this field. First, the topic of NFRHT continues to be dominated by theory, and most of the basic predictions related to the tunability, active control, and thermal management of NFRHT remain to be verified. The challenge now is to combine the novel approaches for the measurement of NFRHT, in both microdevices and macroscale systems, with fabrication and nanostructuration techniques to study the near-field thermal radiation in complex systems and make use of it in functional thermal devices. In particular, it is time to demonstrate and evaluate the feasibility of the different potential applications of NFRHT that have been proposed, with special attention to energy conversion ones. Thus, for instance, after the proof of concept of near-field thermophotovoltaics,[59] it is important to critically assess whether this concept can become a viable technology that could compete, e.g., with thermoelectrics in waste heat recovery applications.

In the context of NFRHT, many of the fundamental effects and applications that we have discussed above are actually based on many-body systems (photon Hall effect, transistor, etc.). Moreover, in recent years there has been growing theoretical interest in fundamental questions related to NFRHT many-body effects.[237−241] Once more, however, to our knowledge no many-body system has ever been studied experimentally. We hope that this will change soon and believe that this topic is going to gain momentum in the coming years.

Two-dimensional materials are revolutionizing materials science, and they are also expected to have a deep impact in the field of radiative heat transfer. Actually, NFRHT in systems involving graphene sheets has been theoretically studied in great detail in recent years.[242−251] Special attention has been paid to the possibility of actively controlling the thermal radiation by electrical means, that is, by controlling graphene's chemical potential with a gate that in turn should control the infrared surface plasmon polaritons that are expected to dominate the thermal radiation in graphene. Again, with a notable exception,[20] this topic has not been investigated experimentally. We are sure that RHT between systems incorporating 2D materials will soon become a hot topic within the field of thermal radiation.

The theory of RHT has its own challenges and open problems. We have already mentioned some of them, such as the need for a better understanding of the crossover regime between radiation and conduction at subnanometer gaps and the development of more efficient methods to deal with micro- and nanostructures with complex shapes and material properties and the presence of temperature profiles.[252] A more fundamental question for the theory is related to the ultimate limits of NFRHT. There has been important progress on that front, and Miller and co-workers[253] have put forward shape-independent limits for the spectral radiative heat transfer rate between two closely spaced bodies. This has allowed us to understand that common large-area structures are actually far away from those theoretical limits, and thus, there is still plenty of room to get even larger NFRHT enhancements. At present, however, there are no clear guidelines on how to approach those limits in practice, and more importantly, similar limits for the total radiative heat transfer have not been derived.

The thermal wavelength is inversely proportional to the temperature, and at cryogenic temperatures (below 1 K), it becomes on the order of millimeters or even centimeters. At such low temperatures, even objects separated by macroscopic gaps can be in the near-field regime. Actually, some of the plate−plate experiments (early[140] and new ones[18]) have benefited from the use of low temperatures. However, most of the experiments are done at room temperature. The use of cryogenic temperatures not only can be a practical advantage but also can enable the exploration of a regime where materials are expected to behave very differently than they do at room temperature. For instance, at low temperature phonon polaritons in polar dielectrics are not thermally occupied, and therefore, they do not contribute to the NFRHT. Moreover, in that temperature regime one could also use superconductors as phase-transition materials, which could lead to new types of phenomena.[196]

As discussed in the previous section, Planck's law fails to describe the RHT between subwavelength objects. Thus, in this regard there are plenty of surprises awaiting in this regime, such as super-Planckian far-field RHT,[106,107,236] but also in the near-field. For this reason, it would be highly desirable to

DOI: 10.1021/acsphotonics.8b01031
ACS Photonics 2018, 5, 3896−3915

develop new experimental techniques that can directly or indirectly test the RHT or thermal emission of small objects. Actually, in the context of levitated nanoparticles there has been important progress in this respect.[254]

Maybe the most mature topic in the context of RHT is the study of the far-field thermal emission of extended objects. As discussed above, in this context one can borrow concepts and methods from the field of photonics, and this has led to very rapid progress on this topic. In any case, there is no reason to believe that the pace of this progress will slow down in the coming years, and of course, it remains to be demonstrated that applications like daytime radiative cooling, thermal radiative textiles, and thermophotovoltaics, just to name a few, can become competitive, widely used technologies.

As has been recently said,[255] heat is the new light, and there is little doubt that the field of radiative heat transfer has a bright future. In spite of the remarkable recent progress, it seems clear that the best is yet to come.

AUTHOR INFORMATION

Corresponding Author

*E-mail: juancarlos.cuevas@uam.es.

ORCID

Juan Carlos Cuevas: 0000-0001-7421-0682

Francisco J. García-Vidal: 0000-0003-4354-0982

Notes

The authors declare no competing financial interest.

ACKNOWLEDGMENTS

This work was financially supported by the Spanish MINECO (FIS2017-84057-P, MAT2014-53432-C5-5-R), the Comunidad de Madrid (S2013/MIT-2740), and the European Research Council (ERC-2011-AdG-290981).

REFERENCES

(1) Modest, M. F. *Radiative Heat Transfer*, 3rd ed.; Academic Press: New York, 2013.

(2) Howell, J. R.; Mengüç, M. P.; Siegel, R. *Thermal Radiation Heat Transfer*, 6th ed.; CRC Press: Boca Raton, FL, 2016.

(3) Zhang, Z. M. *Nano/Microscale Heat Transfer*; McGraw-Hill: New York, 2007.

(4) Planck, M. *The Theory of Thermal Radiation*; P. Blakiston Son & Co.: Philadelphia, 1914.

(5) Joulain, K.; Mulet, J.-P.; Marquier, F.; Carminati, R.; Greffet, J.-J. Surface electromagnetic waves thermally excited: radiative heat transfer, coherence properties and casimir forces revisited in the near field. *Surf. Sci. Rep.* **2005**, *57*, 59−112.

(6) Basu, S.; Zhang, Z. M.; Fu, C. J. Review of near-field thermal radiation and its application to energy conversion. *Int. J. Energy Res.* **2009**, *33*, 1203−1232.

(7) Song, B.; Fiorino, A.; Meyhofer, E.; Reddy, P. Near-field radiative thermal transport: from theory to experiment. *AIP Adv.* **2015**, *5*, 053503.

(8) Polder, D.; Van Hove, M. Theory of radiative heat transfer between closely spaced bodies. *Phys. Rev. B: Condens. Matter Mater. Phys.* **1971**, *4*, 3303−3314.

(9) Rytov, S. M. *Theory of Electric Fluctuations and Thermal Radiation*; Air Force Cambridge Research Center: Bedford, MA, 1953.

(10) Rytov, S. M.; Kravtsov, Y. A.; Tatarskii, V. I. *Principles of Statistical Radiophysics 3: Elements of Random Fields*; Springer: Berlin, 1989.

(11) Kittel, A.; Müller-Hirsch, W.; Parisi, J.; Biehs, S.-A.; Reddig, D.; Holthaus, M. Near-field heat transfer in a scanning thermal microscope. *Phys. Rev. Lett.* **2005**, *95*, 224301.

(12) Hu, L.; Narayanaswamy, A.; Chen, X. Y.; Chen, G. Near-field thermal radiation between two closely spaced glass plates exceeding Planck's blackbody radiation law. *Appl. Phys. Lett.* **2008**, *92*, 133106.

(13) Narayanaswamy, A.; Shen, S.; Chen, G. Near-field radiative heat transfer between a sphere and a substrate. *Phys. Rev. B: Condens. Matter Mater. Phys.* **2008**, *78*, 115303.

(14) Rousseau, E.; Siria, A.; Jourdan, G.; Volz, S.; Comin, F.; Chevrier, J.; Greffet, J.-J. Radiative heat transfer at the nanoscale. *Nat. Photonics* **2009**, *3*, 514−517.

(15) Shen, S.; Narayanaswamy, A.; Chen, G. Surface phonon polaritons mediated energy transfer between nanoscale gaps. *Nano Lett.* **2009**, *9*, 2909−2913.

(16) Ottens, R. S.; Quetschke, V.; Wise, S.; Alemi, A. A.; Lundock, R.; Mueller, G.; Reitze, D. H.; Tanner, D. B.; Whiting, B. F. Near-field radiative heat transfer between macroscopic planar surfaces. *Phys. Rev. Lett.* **2011**, *107*, 014301.

(17) Shen, S.; Mavrokefalos, A.; Sambegoro, P.; Chen, G. Nanoscale thermal radiation between two gold surfaces. *Appl. Phys. Lett.* **2012**, *100*, 233114.

(18) Kralik, T.; Hanzelka, P.; Zobac, M.; Musilova, V.; Fort, T.; Horak, M. Strong near-field enhancement of radiative heat transfer between metallic surfaces. *Phys. Rev. Lett.* **2012**, *109*, 224302.

(19) van Zwol, P. J.; Ranno, L.; Chevrier, J. Tuning near field radiative heat flux through surface excitations with a metal insulator transition. *Phys. Rev. Lett.* **2012**, *108*, 234301.

(20) van Zwol, P.-J.; Thiele, S.; Berger, C.; de Heer, W. A.; Chevrier, J. Nanoscale radiative heat flow due to surface plasmons in graphene and doped silicon. *Phys. Rev. Lett.* **2012**, *109*, 264301.

(21) Guha, B.; Otey, C.; Poitras, C. B.; Fan, S. H.; Lipson, M. Near-field radiative cooling of nanostructures. *Nano Lett.* **2012**, *12*, 4546−4550.

(22) Worbes, L.; Hellmann, D.; Kittel, A. Enhanced near-field heat flow of a monolayer dielectric island. *Phys. Rev. Lett.* **2013**, *110*, 134302.

(23) Shi, J.; Li, P.; Liu, B.; Shen, S. Tuning near field radiation by doped silicon. *Appl. Phys. Lett.* **2013**, *102*, 183114.

(24) St-Gelais, R.; Guha, B.; Zhu, L. X.; Fan, S.; Lipson, M. Demonstration of strong near-field radiative heat transfer between integrated nanostructures. *Nano Lett.* **2014**, *14*, 6971−6975.

(25) Song, B.; Ganjeh, Y.; Sadat, S.; Thompson, D.; Fiorino, A.; Fernández-Hurtado, V.; Feist, J.; Garcia-Vidal, F. J.; Cuevas, J. C.; Reddy, P.; Meyhofer, E. Enhancement of near-field radiative heat transfer using polar dielectric thin films. *Nat. Nanotechnol.* **2015**, *10*, 253−258.

(26) Kim, K.; Song, B.; Fernández-Hurtado, V.; Lee, W.; Jeong, W.; Cui, L.; Thompson, D.; Feist, J.; Reid, M. T. H.; Garcia-Vidal, F. J.; Cuevas, J. C.; Meyhofer, E.; Reddy, P. Radiative heat transfer in the extreme near field. *Nature* **2015**, *528*, 387−391.

(27) Lim, M.; Lee, S. S.; Lee, B. J. Near-field thermal radiation between doped silicon plates at nanoscale gaps. *Phys. Rev. B: Condens. Matter Mater. Phys.* **2015**, *91*, 195136.

(28) St-Gelais, R.; Zhu, L.; Fan, S.; Lipson, M. Near-field radiative heat transfer between parallel structures in the deep subwavelength regime. *Nat. Nanotechnol.* **2016**, *11*, 515−519.

(29) Song, B.; Thompson, D.; Fiorino, A.; Ganjeh, Y.; Reddy, P.; Meyhofer, E. Radiative heat conductances between dielectric and metallic parallel plates with nanoscale gaps. *Nat. Nanotechnol.* **2016**, *11*, 509−514.

(30) Bernardi, M. P.; Milovich, D.; Francoeur, M. Radiative heat transfer exceeding the blackbody limit between macroscale planar surfaces separated by a nanosize vacuum gap. *Nat. Commun.* **2016**, *7*, 12900.

(31) Cui, L.; Jeong, W.; Fernández-Hurtado, V.; Feist, J.; García-Vidal, F. J.; Cuevas, J. C.; Meyhofer, E.; Reddy, P. Study of radiative heat transfer in Ångström- and nanometre-sized gaps. *Nat. Commun.* **2017**, *8*, 14479.

(32) Kloppstech, K.; Könne, N.; Biehs, S.-A.; Rodriguez, A. W.; Worbes, L.; Hellmann, D.; Kittel, A. Giant heat transfer in the

DOI: 10.1021/acsphotonics.8b01031
ACS Photonics 2018, 5, 3896−3915

crossover regime between conduction and radiation. *Nat. Commun.* **2017**, *8*, 14475.
(33) Ghashami, M.; Geng, H.; Kim, T.; Iacopino, N.; Cho, S.-K.; Park, K. Precision measurement of phonon-polaritonic near-field energy transfer between macroscale planar structures under large thermal gradients. *Phys. Rev. Lett.* **2018**, *120*, 175901.
(34) Fiorino, A.; Thompson, D.; Zhu, L.; Song, B.; Reddy, P.; Meyhofer, E. Giant enhancement in radiative heat transfer in sub-30 nm gaps of plane parallel surfaces. *Nano Lett.* **2018**, *18*, 3711−3715.
(35) Challener, W. A.; Peng, C. B.; Itagi, A. V.; Karns, D.; Peng, W.; Peng, Y. Y.; Yang, X. M.; Zhu, X. B.; Gokemeijer, N. J.; Hsia, Y. T.; Ju, G.; Rottmayer, R. E.; Seigler, M. A.; Gage, E. C. Heat-assisted magnetic recording by a near-field transducer with efficient optical energy transfer. *Nat. Photonics* **2009**, *3*, 220−224.
(36) Stipe, B. C.; Strand, T. C.; Poon, C. C.; Balamane, H.; Boone, T. D.; Katine, J. A.; Li, J. L.; Rawat, V.; Nemoto, H.; Hirotsune, A.; Hellwig, O.; Ruiz, R.; Dobisz, E.; Kercher, D. S.; Robertson, N.; Albrecht, T. R.; Terris, B. D. Terris. Magnetic recording at 1.5 Pb m^2 using an integrated plasmonic antenna. *Nat. Photonics* **2010**, *4*, 484−488.
(37) Pendry, J. B. Radiative exchange of heat between nanostructures. *J. Phys.: Condens. Matter* **1999**, *11*, 6621−6633.
(38) De Wilde, Y.; Formanek, F.; Carminati, R.; Gralak, B.; Lemoine, P. A.; Joulain, K.; Mulet, J. P.; Chen, Y.; Greffet, J. J. Thermal radiation scanning tunnelling microscopy. *Nature* **2006**, *444*, 740−743.
(39) Kittel, A.; Wischnath, U. F.; Welker, J.; Huth, O.; Ruting, F.; Biehs, S. A. Near-field thermal imaging of nanostructured surfaces. *Appl. Phys. Lett.* **2008**, *93*, 193109.
(40) Jones, A. C.; O'Callahan, B. T.; Yang, H. U.; Raschke, M. B. The thermal near-field: Coherence, spectroscopy, heat transfer, and optical forces. *Prog. Surf. Sci.* **2013**, *88*, 349−392.
(41) Carminati, R.; Greffet, J. J. Near-field effects in spatial coherence of thermal sources. *Phys. Rev. Lett.* **1999**, *82*, 1660−1663.
(42) Greffet, J. J.; Carminati, R.; Joulain, K.; Mulet, J. P.; Mainguy, S. P.; Chen, Y. Coherent emission of light by thermal sources. *Nature* **2002**, *416*, 61−64.
(43) Otey, C.; Lau, W. T.; Fan, S. Thermal rectification through vacuum. *Phys. Rev. Lett.* **2010**, *104*, 154301.
(44) Ben-Abdallah, P.; Biehs, S. A. Near-field thermal transistor. *Phys. Rev. Lett.* **2014**, *112*, 044301.
(45) Fiorino, A.; Thompson, D.; Zhu, L.; Mittapally, R.; Biehs, S.-A.; Bezencenet, O.; El-Bondry, N.; Bansropun, S.; Ben-Abdallah, P.; Meyhofer, E.; Reddy, P. A thermal diode based on nanoscale thermal radiation. *ACS Nano* **2018**, *12*, 5774−5779.
(46) Whale, M. D.; Cravalho, E. G. Modeling and performance of microscale thermophotovoltaic energy conversion devices. *IEEE Trans. Energy Conver.* **2002**, *17*, 130−142.
(47) Narayanaswamy, A.; Chen, G. Surface modes for near field thermophotovoltaics. *Appl. Phys. Lett.* **2003**, *82*, 3544−3546.
(48) Laroche, M.; Carminati, R.; Greffet, J. J. Near-field thermophotovoltaic energy conversion. *J. Appl. Phys.* **2006**, *100*, 063704.
(49) Basu, S.; Chen, Y. B.; Zhang, Z. M. Microscale radiation in thermophotovoltaic devices—a review. *Int. J. Energy Res.* **2007**, *31*, 689−716.
(50) Park, K.; Basu, S.; King, W. P.; Zhang, Z. M. Performance analysis of near-field thermophotovoltaic devices considering absorption distribution. *J. Quant. Spectrosc. Radiat. Transfer* **2008**, *109*, 305−316.
(51) Francoeur, M.; Vaillon, R.; Mengüç, M. P. Thermal impacts on the performance of nanoscale-gap thermophotovoltaic power generators. *IEEE Transactions on Energy Conversion* **2011**, *26*, 686−698.
(52) Messina, R.; Ben-Abdallah, P. Graphene-based photovoltaic cells for near-field thermal energy conversion. *Sci. Rep.* **2013**, *3*, 1383.
(53) Bright, T. J.; Wang, L. P.; Zhang, Z. M. Performance of near-field thermophotovoltaic cells enhanced with a backside reflector. *J. Heat Transfer* **2014**, *136*, 062701.
(54) Bernardi, M. P.; Dupré, O.; Blandre, E.; Chapuis, P. O.; Vaillon, R.; Francoeur, M. Impacts of propagating, frustrated and surface modes on radiative, electrical and thermal losses in nanoscale-gap thermophotovoltaic power generators. *Sci. Rep.* **2015**, *5*, 11626.
(55) Tong, J. K.; Hsu, W. C.; Huang, Y.; Boriskina, S. V.; Chen, G. Thin-film "thermal well" emitters and absorbers for high-efficiency thermophotovoltaics. *Sci. Rep.* **2015**, *5*, 10661.
(56) Chen, K. F.; Santhanam, P.; Fan, S. Suppressing sub-bandgap phonon-polariton heat transfer in near-field thermophotovoltaic devices for waste heat recovery. *Appl. Phys. Lett.* **2015**, *107*, 091106.
(57) Lau, J. Z. J.; Wong, B. T. Thermal energy conversion using near-field thermophotovoltaic device composed of a thin-film tungsten radiator and a thin-film silicon cell. *J. Appl. Phys.* **2017**, *122*, 084302.
(58) Zhao, B.; Chen, K.; Buddhiraju, S.; Bhatt, G.; Lipson, M.; Fan, S. High-performance near-field thermophotovoltaics for waste heat recovery. *Nano Energy* **2017**, *41*, 344−350.
(59) Fiorino, A.; Zhu, L.; Thompson, D.; Mittapally, R.; Reddy, P.; Meyhofer, E. Nanogap near-field thermophotovoltaics. *Nat. Nanotechnol.* **2018**, *13*, 806.
(60) Schwede, J. W.; Bargatin, I.; Riley, D. C.; Hardin, B. E.; Rosenthal, S. J.; Sun, Y.; Schmitt, F.; Pianetta, P.; Howe, R. T.; Shen, Z. X.; Melosh, N. A. Photon-enhanced thermionic emission for solar concentrator systems. *Nat. Mater.* **2010**, *9*, 762−767.
(61) Chen, K.; Santhanam, P.; Sandhu, S.; Zhu, L.; Fan, S. Heat-flux control and solid-state cooling by regulating chemical potential of photons in near-field electromagnetic heat transfer. *Phys. Rev. B: Condens. Matter Mater. Phys.* **2015**, *91*, 134301.
(62) Chen, K.; Santhanam, P.; Fan, S. Near-field enhanced negative luminescent refrigeration. *Phys. Rev. Appl.* **2016**, *6*, 024014.
(63) Li, W.; Fan, S. Nanophotonic control of thermal radiation for energy applications. *Opt. Express* **2018**, *26*, 15995−16021.
(64) Liu, X.; Tyler, T.; Starr, T.; Starr, A. F.; Jokerst, N. M.; Padilla, W. J. Taming the blackbody with infrared metamaterials as selective thermal emitters. *Phys. Rev. Lett.* **2011**, *107*, 045901.
(65) De Zoysa, M.; Asano, T.; Mochizuki, K.; Oskooi, A.; Inoue, T.; Noda, S. Conversion of broadband to narrowband thermal emission through energy recycling. *Nat. Photonics* **2012**, *6*, 535−539.
(66) Guo, Y.; Fan, S. Narrowband thermal emission from a uniform tungsten surface critically coupled with a photonic crystal guided resonance. *Opt. Express* **2016**, *24*, 29896−29907.
(67) Liu, B.; Gong, W.; Yu, B.; Li, P.; Shen, S. Perfect thermal emission by nanoscale transmission line resonators. *Nano Lett.* **2017**, *17*, 666−672.
(68) Chan, D. L. C.; Soljačić, M.; Joannopoulos, J. D. Thermal emission and design in one-dimensional periodic metallic photonic crystal slabs. *Phys. Rev. E: Stat. Nonlin. Soft Matter Phys.* **2006**, *74*, 016609.
(69) Miyazaki, H. T.; Ikeda, K.; Kasaya, T.; Yamamoto, K.; Inoue, Y.; Fujimura, K.; Kanakugi, T.; Okada, M.; Hatade, K.; Kitagawa, S. Thermal emission of two-color polarized infrared waves from integrated plasmon cavities. *Appl. Phys. Lett.* **2008**, *92*, 141114.
(70) Schuller, J. A.; Taubner, T.; Brongersma, M. L. Optical antenna thermal emitters. *Nat. Photonics* **2009**, *3*, 658−661.
(71) Laroche, M.; Arnold, C.; Marquier, F.; Carminati, R.; Greffet, J.-J.; Collin, S.; Bardou, N.; Pelouard, J.-L. Highly directional radiation generated by a tungsten thermal source. *Opt. Lett.* **2005**, *30*, 2623−2625.
(72) Laroche, M.; Carminati, R.; Greffet, J.-J. Coherent thermal antenna using a photonic crystal slab. *Phys. Rev. Lett.* **2006**, *96*, 123903.
(73) Han, S. E.; Norris, D. J. Beaming thermal emission from hot metallic bull's eyes. *Opt. Express* **2010**, *18*, 4829−4837.
(74) Kosten, E. D.; Atwater, J. H.; Parsons, J.; Polman, A.; Atwater, H. A. Highly efficient GaAs solar cells by limiting light emission angle. *Light: Sci. Appl.* **2013**, *2*, e45.
(75) Shen, Y.; Ye, D.; Celanovic, I.; Johnson, S. G.; Joannopoulos, J. D.; Soljačić, M. Optical broadband angular selectivity. *Science* **2014**, *343*, 1499−1501.

DOI: 10.1021/acsphotonics.8b01031
ACS Photonics 2018, 5, 3896−3915

(76) Park, J. H.; Han, S. E.; Nagpal, P.; Norris, D. J. Observation of thermal beaming from tungsten and molybdenum bull's eyes. *ACS Photonics* **2016**, *3*, 494−500.
(77) Chalabi, H.; Alù, A.; Brongersma, M. L. Focused thermal emission from a nanostructured SiC surface. *Phys. Rev. B: Condens. Matter Mater. Phys.* **2016**, *94*, 094307.
(78) Rephaeli, E.; Raman, A.; Fan, S. Ultrabroadband photonic structures to achieve high-performance daytime radiative cooling. *Nano Lett.* **2013**, *13*, 1457−1461.
(79) Raman, A. P.; Anoma, M. A.; Zhu, L.; Rephaeli, E.; Fan, S. Passive radiative cooling below ambient air temperature under direct sunlight. *Nature* **2014**, *515*, 540−544.
(80) Hossain, M. M.; Jia, B.; Gu, M. A metamaterial emitter for highly efficient radiative cooling. *Adv. Opt. Mater.* **2015**, *3*, 1047−1051.
(81) Gentle, A. R.; Smith, G. B. A subambient open roof surface under the mid-summer Sun. *Adv. Sci.* **2015**, *2*, 1500119.
(82) Chen, Z.; Zhu, L.; Raman, A.; Fan, S. Radiative cooling to deep sub-freezing temperatures through a 24-h day-night cycle. *Nat. Commun.* **2016**, *7*, 13729.
(83) Kou, J.; Jurado, Z.; Chen, Z.; Fan, S.; Minnich, A. J. Daytime radiative cooling using near-black infrared emitters. *ACS Photonics* **2017**, *4*, 626−630.
(84) Zhai, Y.; Ma, Y.; David, S. N.; Zhao, D.; Lou, R.; Tan, G.; Yang, R.; Yin, X. Scalable-manufactured randomized glass-polymer hybrid metamaterial for daytime radiative cooling. *Science* **2017**, *355*, 1062−1066.
(85) Goldstein, E. A.; Raman, A. P.; Fan, S. Sub-ambient non-evaporative fluid cooling with the sky. *Nat. Energy* **2017**, *2*, 17143.
(86) Tong, J. K.; Huang, X.; Boriskina, S. V.; Loomis, J.; Xu, Y.; Chen, Y. Infrared-transparent visible-opaque fabrics for wearable personal thermal management. *ACS Photonics* **2015**, *2*, 769−778.
(87) Hsu, P. C.; Liu, X.; Liu, C.; Xie, X.; Lee, H. R.; Welch, A. J.; Zhao, T.; Cui, Y. Personal thermal management by metallic nanowire-coated textile. *Nano Lett.* **2015**, *15*, 365−371.
(88) Hsu, P. C.; Song, A. Y.; Catrysse, P. B.; Liu, C.; Peng, Y.; Xie, J.; Fan, S.; Cui, Y. Radiative human body cooling by nanoporous polyethylene textile. *Science* **2016**, *353*, 1019−1023.
(89) Catrysse, P. B.; Song, A. Y.; Fan, S. Photonic structure textile design for localized thermal cooling based on a fiber blending scheme. *ACS Photonics* **2016**, *3*, 2420−2426.
(90) Yang, A.; Cai, L.; Zhang, R.; Wang, J.; Hsu, P. C.; Wang, H.; Zhou, G.; Xu, J.; Cui, Y. Thermal management in nanofiber-based face mask. *Nano Lett.* **2017**, *17*, 3506−3510.
(91) Cai, L.; Song, A. Y.; Wu, P.; Hsu, P. C.; Peng, Y.; Chen, J.; Liu, C.; Catrysse, P. B.; Liu, Y.; Yang, A.; Zhou, C.; Zhou, C.; Fan, S.; Cui, Y. Warming up human body by nanoporous metallized polyethylene textile. *Nat. Commun.* **2017**, *8*, 496.
(92) Hsu, P. C.; Liu, C.; Song, A. Y.; Zhang, Z.; Peng, Y.; Xie, J.; Liu, K.; Wu, C.-L.; Catrysse, P. B.; Cai, L.; Zhai, S.; Majumdar, A.; Fan, S.; Cui, Y. A dual-mode textile for human body radiative heating and cooling. *Sci. Adv.* **2017**, *3*, e1700895.
(93) Jafar-Zanjani, S.; Salary, M. M.; Mosallaei, H. Metafabrics for thermoregulation and energy-harvesting applications. *ACS Photonics* **2017**, *4*, 915−927.
(94) Gao, T.; Yang, Z.; Chen, C.; Li, Y.; Fu, K.; Dai, J.; Hitz, E. M.; Xie, H.; Liu, B.; Song, J.; Yang, B.; Hu, L. Three-dimensional printed thermal regulation textiles. *ACS Nano* **2017**, *11*, 11513−11520.
(95) Zhu, L.; Raman, A.; Wang, K. X.; Anoma, M. A.; Fan, S. Radiative cooling of solar cells. *Optica* **2014**, *1*, 32−38.
(96) Zhu, L.; Raman, A. P.; Fan, S. Radiative cooling of solar absorbers using a visibly transparent photonic crystal thermal blackbody. *Proc. Natl. Acad. Sci. U. S. A.* **2015**, *112*, 12282−12287.
(97) Li, W.; Shi, Y.; Chen, K.; Zhu, L.; Fan, S. A comprehensive photonic approach for solar cell cooling. *ACS Photonics* **2017**, *4*, 774−782.
(98) Lenert, A.; Bierman, D. M.; Nam, Y.; Chan, W. R.; Celanović, I.; Soljačić, M.; Wang, E. N. A nanophotonic solar thermophotovoltaic device. *Nat. Nanotechnol.* **2014**, *9*, 126−130.
(99) Bierman, D. M.; Lenert, A.; Chan, W. R.; Bhatia, B.; Celanović, I.; Soljačić, M.; Wang, E. N. Enhanced photovoltaic energy conversion using thermally based spectral shaping. *Nat. Energy* **2016**, *1*, 16068.
(100) Zhu, L.; Fan, S. Near-complete violation of detailed balance in thermal radiation. *Phys. Rev. B: Condens. Matter Mater. Phys.* **2014**, *90*, 220301.
(101) Biehs, S.-A.; Ben-Abdallah, P. Revisiting super-Planckian thermal emission in the far-field regime. *Phys. Rev. B: Condens. Matter Mater. Phys.* **2016**, *93*, 165405.
(102) Bohren, C. F.; Huffman, D. R. *Absorption and Scattering of Light by Small Particles*; Wiley: New York, 1998.
(103) Kattawar, G. W.; Eisner, M. Radiation from a homogeneous isothermal sphere. *Appl. Opt.* **1970**, *9*, 2685−2690.
(104) Golyk, V. A.; Krüger, M.; Kardar, M. Heat radiation from long cylindrical objets. *Phys. Rev. E: Stat. Nonlin. Soft Matter Phys.* **2012**, *85*, 046603.
(105) Maslovski, S. I.; Simovski, C. R.; Tretyakov, S. A. Overcoming blackbody radiation limit in free space: metamaterial superemitter. *New J. Phys.* **2016**, *18*, 013034.
(106) Fernández-Hurtado, V.; Fernández-Domínguez, A. I.; Feist, J.; García-Vidal, F. J.; Cuevas, J. C. Super-Planckian far-field radiative heat transfer. *Phys. Rev. B: Condens. Matter Mater. Phys.* **2018**, *97*, 045408.
(107) Fernández-Hurtado, V.; Fernández-Domínguez, A. I.; Feist, J.; García-Vidal, F. J.; Cuevas, J. C. Exploring the limits of Super-Planckian far-field radiative heat transfer using 2D materials. *ACS Photonics* **2018**, *5*, 3082−3088.
(108) Chapuis, P. O.; Volz, S.; Henkel, C.; Joulain, K.; Greffet, J.-J. Effects of spatial dispersion in near-field radiative heat transfer between two parallel metallic surfaces. *Phys. Rev. B: Condens. Matter Mater. Phys.* **2008**, *77*, 035431.
(109) Mulet, J. P.; Joulain, K.; Carminati, R.; Greffet, J.-J. Enhanced radiative heat transfer at nanometric distances. *Microscale Thermophys. Eng.* **2002**, *6*, 209−222.
(110) Landau, L.; Lifshitz, E.; Pitaevskii, L. *Course of Theoretical Physics*; Pergamon Press: New York, 1980; Vol. *9*, Part 2.
(111) Il'inskii, Yu. A.; Keldysh, L. V. *Electromagnetic Response of Material Media*; Plenum Press: New York, 1994.
(112) Narayanaswamy, A.; Chen, G. Thermal near-field radiative transfer between two spheres. *Phys. Rev. B: Condens. Matter Mater. Phys.* **2008**, *77*, 075125.
(113) Otey, C. R.; Fan, S. Numerically exact calculation of electromagnetic heat transfer between a dielectric sphere and plate. *Phys. Rev. B: Condens. Matter Mater. Phys.* **2011**, *84*, 245431.
(114) Otey, C. R.; Zhu, L.; Sandhu, S.; Fan, S. Fluctuational electrodynamics calculations of near- field heat transfer in non-planar geometries: A brief overview. *J. Quant. Spectrosc. Radiat. Transfer* **2014**, *132*, 3−11.
(115) Francoeur, M.; Mengüç, M. P. Role of fluctuational electrodynamics in near-field radiative heat transfer. *J. Quant. Spectrosc. Radiat. Transfer* **2008**, *109*, 280−293.
(116) Francoeur, M.; Mengüç, M. P.; Vaillon, R. Solution of near-field thermal radiation in one-dimensional layered media using dyadic Green's functions and the scattering matrix method. *J. Quant. Spectrosc. Radiat. Transfer* **2009**, *110*, 2002−2018.
(117) Ben-Abdallah, P.; Joulain, K.; Pryamikov, A. Surface Bloch waves mediated heat transfer between two photonic crystals. *Appl. Phys. Lett.* **2010**, *96*, 143117.
(118) Zheng, Z.; Xuan, Y. Theory of near-field radiative heat transfer for stratified magnetic media. *Int. J. Heat Mass Transfer* **2011**, *54*, 1101−1110.
(119) Bimonte, G. Scattering approach to Casimir forces and radiative heat transfer for nanostructured surfaces out of thermal equilibrium. *Phys. Rev. A: At., Mol., Opt. Phys.* **2009**, *80*, 042102.
(120) Messina, R.; Antezza, M. Scattering-matrix approach to Casimir−Lifshitz force and heat transfer out of thermal equilibrium between arbitrary bodies. *Phys. Rev. A: At., Mol., Opt. Phys.* **2011**, *84*, 042102.

DOI: 10.1021/acsphotonics.8b01031
ACS Photonics 2018, 5, 3896−3915

(121) Krüger, M.; Emig, T.; Kardar, M. Nonequilibrium electromagnetic fluctuations: Heat transfer and interactions. *Phys. Rev. Lett.* **2011**, *106*, 210404.
(122) Krüger, M.; Bimonte, G.; Emig, T.; Kardar, M. Trace formulas for nonequilibrium Casimir interactions, heat radiation, and heat transfer for arbitrary objects. *Phys. Rev. B: Condens. Matter Mater. Phys.* **2012**, *86*, 115423.
(123) Rodriguez, A. W.; Ilic, O.; Bermel, P.; Celanović, I.; Joannopoulos, J. D.; Soljačić, M.; Johnson, S. G. Frequency-selective near-field radiative heat transfer between photonic crystal slabs: A computational approach for arbitrary geometries and materials. *Phys. Rev. Lett.* **2011**, *107*, 114302.
(124) Liu, B.; Shen, S. Broadband near-field radiative thermal emitter/absorber based on hyperbolic metamaterials: Direct numerical simulation by the Wiener chaos expansion method. *Phys. Rev. B: Condens. Matter Mater. Phys.* **2013**, *87*, 115403.
(125) Datas, A.; Hirashima, D.; Hanamura, K. FDTD simulation of near-field radiative heat transfer between thin films supporting surface phonon polaritons: Lessons learned. *J. Therm. Sci. Technol.* **2013**, *8*, 91−105.
(126) Wen, S. B. Direct numerical simulation of near field thermal radiation based on Wiener chaos expansion of thermal fluctuating current. *J. Heat Transfer* **2010**, *132*, 072704.
(127) Rodriguez, A. W.; Reid, M. T. H.; Johnson, S. G. Fluctuating-surface-current formulation of radiative heat transfer for arbitrary geometries. *Phys. Rev. B: Condens. Matter Mater. Phys.* **2012**, *86*, 220302.
(128) Rodriguez, A. W.; Reid, M. T. H.; Johnson, S. G. Fluctuating-surface-current formulation of radiative heat transfer: theory and applications. *Phys. Rev. B: Condens. Matter Mater. Phys.* **2013**, *88*, 054305.
(129) Reid, M. T. H.; Johnson, S. G. Efficient computation of power, force and torque in BEM scattering calculations. *IEEE Trans. Antennas Propag.* **2015**, *63*, 3588−3598.
(130) Polimeridis, A. G.; Reid, M. T. H.; Jin, W.; Johnson, S. G.; White, J. K.; Rodriguez, A. W. Fluctuating volume-current formulation of electromagnetic fluctuations in inhomogeneous media: Incandescence and luminescence in arbitrary geometries. *Phys. Rev. B: Condens. Matter Mater. Phys.* **2015**, *92*, 134202.
(131) Edalatpour, S.; Francoeur, M. The Thermal Discrete Dipole Approximation (T-DDA) for near-field radiative heat transfer simulations in three-dimensional arbitrary geometries. *J. Quant. Spectrosc. Radiat. Transfer* **2014**, *133*, 364−373.
(132) Edalatpour, S.; Cuma, M.; Trueax, T.; Backman, R.; Francoeur, M. Convergence analysis of the thermal discrete dipole approximation. *Phys. Rev. E: Stat. Nonlin. Soft Matter Phys.* **2015**, *91*, 063307.
(133) Abraham Ekeroth, R. M.; García-Martín, A.; Cuevas, J. C. Thermal discrete dipole approximation for the description of thermal emission and radiative heat transfer of magneto-optical systems. *Phys. Rev. B: Condens. Matter Mater. Phys.* **2017**, *95*, 235428.
(134) Singer, F.; Ezzahri, Y.; Joulain, K. Near field radiative heat transfer between two nonlocal dielectrics. *J. Quant. Spectrosc. Radiat. Transfer* **2015**, *154*, 55−62.
(135) Xiong, S.; Yang, K.; Kosevich, Y. A.; Chalopin, Y.; D'Agosta, R.; Cortona, P.; Volz, S. Classical to quantum transition of heat transfer between two silica clusters. *Phys. Rev. Lett.* **2014**, *112*, 114301.
(136) Klöckner, J. C.; Siebler, R.; Cuevas, J. C.; Pauly, F. Thermal conductance and thermoelectric figure of merit of C_{60}-based single-molecule junctions: electrons, phonons, and photons. *Phys. Rev. B: Condens. Matter Mater. Phys.* **2017**, *95*, 245404.
(137) Chiloyan, V.; Garg, J.; Esfarjani, K.; Chen, G. Transition from near-field thermal radiation to phonon heat conduction at sub-nanometre gaps. *Nat. Commun.* **2015**, *6*, 6755.
(138) Cravalho, E. G.; Domoto, G. A.; Tien, C. L. Presented at the AIAA 3rd Thermophysics Conference, Los Angeles, CA, 1968.
(139) Hargreaves, C. M. Anomalous radiative transfer between closely-spaced bodies. *Phys. Lett. A* **1969**, *30*, 491−492.
(140) Domoto, G. A.; Boehm, R. F.; Tien, C. L. Experimental investigation of radiative transfer between metallic surfaces at cryogenic temperatures. *J. Heat Transfer* **1970**, *92*, 412−416.
(141) Jones, A. C.; Raschke, M. B. Thermal infrared near-field spectroscopy. *Nano Lett.* **2012**, *12*, 1475−1481.
(142) Zhang, L. M.; Andreev, G. O.; Fei, Z.; McLeod, A. S.; Domínguez, G.; Thiemens, M.; Castro-Neto, A. H.; Basov, D. N.; Fogler, M. M. Near-field spectroscopy of silicon dioxide thin films. *Phys. Rev. B: Condens. Matter Mater. Phys.* **2012**, *85*, 075419.
(143) Babuty, A.; Joulain, K.; Chapuis, P. O.; Greffet, J.-J.; De Wilde, Y. Blackbody spectrum revisited in the near field. *Phys. Rev. Lett.* **2013**, *110*, 146103.
(144) O'Callahan, B. T.; Lewis, W. E.; Jones, A. C.; Raschke, M. B. Spectral frustration and spatial coherence in thermal near-field spectroscopy. *Phys. Rev. B: Condens. Matter Mater. Phys.* **2014**, *89*, 245446.
(145) Peragut, F.; Brubach, J. B.; Roy, P.; De Wilde, Y. Infrared near-field imaging and spectroscopy based on thermal or synchrotron radiation. *Appl. Phys. Lett.* **2014**, *104*, 251118.
(146) Joulain, K.; Ben-Abdallah, P.; Chapuis, P. O.; De Wilde, Y.; Babuty, A.; Henkel, C. Strong tip-sample coupling in thermal radiation scanning tunneling microscopy. *J. Quant. Spectrosc. Radiat. Transfer* **2014**, *136*, 1−15.
(147) Cui, L.; Jeong, W.; Hur, S.; Matt, M.; Klöckner, J. C.; Pauly, F.; Nielaba, P.; Cuevas, J. C.; Meyhofer, E.; Reddy, P. Quantized thermal transport in single-atom junctions. *Science* **2017**, *355*, 1192−1195.
(148) Mosso, N.; Drechsler, U.; Menges, F.; Nirmalraj, P.; Karg, S.; Riel, H.; Gotsmann, B. Heat transport through atomic contacts. *Nat. Nanotechnol.* **2017**, *12*, 430−433.
(149) Klöckner, J. C.; Matt, M.; Nielaba, P.; Pauly, F.; Cuevas, J. C. Thermal conductance of metallic atomic-size contacts: Phonon transport and Wiedemann−Franz law. *Phys. Rev. B: Condens. Matter Mater. Phys.* **2017**, *96*, 205405.
(150) Francoeur, M.; Mengüç, M. P.; Vaillon, R. Near-field radiative heat transfer enhancement via surface phonon polaritons coupling in thin films. *Appl. Phys. Lett.* **2008**, *93*, 043109.
(151) Ben-Abdallah, P.; Joulain, K.; Drevillon, J.; Domingues, G. Near-field heat transfer mediated by surface wave hybridization between two films. *J. Appl. Phys.* **2009**, *106*, 044306.
(152) Francoeur, M.; Mengüç, M. P.; Vaillon, R. Spectral tuning of near-field radiative heat flux between two thin silicon carbide films. *J. Phys. D: Appl. Phys.* **2010**, *43*, 075501.
(153) Basu, S.; Francoeur, M. Maximum near-field radiative heat transfer between thin films. *Appl. Phys. Lett.* **2011**, *98*, 243120.
(154) Francoeur, M.; Mengüç, M. P.; Vaillon, R. Coexistence of multiple regimes for near-field thermal radiation between two layers supporting surface phonon polaritons in the infrared. *Phys. Rev. B: Condens. Matter Mater. Phys.* **2011**, *84*, 075436.
(155) Miller, O. D.; Johnson, S. G.; Rodriguez, A. W. Effectiveness of thin films in lieu of hyperbolic metamaterials in the near field. *Phys. Rev. Lett.* **2014**, *112*, 157402.
(156) Jin, W.; Messina, R.; Rodriguez, A. W. Overcoming limits to near-field radiative heat transfer in uniform planar media through multilayer optimization. *Opt. Express* **2017**, *25*, 14746−14759.
(157) Iizuka, H.; Fan, S. Significant enhancement of near-field electromagnetic heat transfer in a multilayer structure through multiple surface-states coupling. *Phys. Rev. Lett.* **2018**, *120*, 063901.
(158) Nefedov, I. S.; Simovski, C. R. Giant radiation heat transfer through micron gaps. *Phys. Rev. B: Condens. Matter Mater. Phys.* **2011**, *84*, 195459.
(159) Biehs, S. A.; Tschikin, M.; Ben-Abdallah, P. Hyperbolic metamaterials as an analog of a blackbody in the near field. *Phys. Rev. Lett.* **2012**, *109*, 104301.
(160) Guo, Y.; Cortes, C. L.; Molesky, S.; Jacob, Z. Broadband super-Planckian thermal emission from hyperbolic metamaterials. *Appl. Phys. Lett.* **2012**, *101*, 131106.
(161) Poddubny, A.; Iorsh, I.; Belov, P.; Kivshar, Y. Hyperbolic metamaterials. *Nat. Photonics* **2013**, *7*, 948−957.

DOI: 10.1021/acsphotonics.8b01031
ACS Photonics 2018, 5, 3896−3915

(162) Biehs, S. A.; Tschikin, M.; Messina, R.; Ben-Abdallah, P. Super-Planckian near-field thermal emission with phonon-polaritonic hyperbolic metamaterials. *Appl. Phys. Lett.* **2013**, *102*, 131106.
(163) Tschikin, M.; Biehs, S. A.; Messina, R.; Ben-Abdallah, P. On the Limits of the effective description of hyperbolic materials in presence of surface waves. *J. Opt.* **2013**, *15*, 105101.
(164) Guo, Y.; Jacob, Z. B. Thermal hyperbolic metamaterials. *Opt. Express* **2013**, *21*, 15014−15019.
(165) Simovski, C.; Maslovski, S.; Nefedov, I.; Tretyakov, S. Optimization of radiative heat transfer in hyperbolic metamaterials for thermophotovoltaic applications. *Opt. Express* **2013**, *21*, 14988−15013.
(166) Liu, X. L.; Zhang, R. Z.; Zhang, Z. M. Near-field thermal radiation between hyperbolic metamaterials: Graphite and carbon nanotubes. *Appl. Phys. Lett.* **2013**, *103*, 213102.
(167) Liu, X. L.; Zhang, R. Z.; Zhang, Z. M. Near-Field radiative heat transfer with doped-silicon nanostructured metamaterials. *Int. J. Heat Mass Transfer* **2014**, *73*, 389−398.
(168) Guo, Y.; Jacob, Z. B. Fluctuational electrodynamics of hyperbolic metamaterials. *J. Appl. Phys.* **2014**, *115*, 234306.
(169) Lang, S.; Tschikin, M.; Biehs, S. A.; Petrov, A. Yu.; Eich, M. Large penetration depth of near-field heat flux in hyperbolic media. *Appl. Phys. Lett.* **2014**, *104*, 121903.
(170) Tschikin, M.; Biehs, S. A.; Ben-Abdallah, P.; Lang, S.; Petrov, A. Yu.; Eich, M. Radiative heat flux predictions in hyperbolic metamaterials. *J. Quant. Spectrosc. Radiat. Transfer* **2015**, *158*, 17−26.
(171) Guérout, R.; Lussange, J.; Rosa, F. S. S.; Hugonin, J.-P.; Dalvit, D. A. R.; Greffet, J. J.; Lambrecht, A.; Reynaud, S. Enhanced radiative heat transfer between nanostructured gold plates. *Phys. Rev. B: Condens. Matter Mater. Phys.* **2012**, *85*, 180301.
(172) Dai, J.; Dyakov, S. A.; Yan, M. Enhanced near-field radiative heat transfer between corrugated metal plates: Role of spoof surface plasmon polaritons. *Phys. Rev. B: Condens. Matter Mater. Phys.* **2015**, *92*, 035419.
(173) Dai, J.; Dyakov, S. A.; Yan, M. Radiative heat transfer between two dielectric-filled metal gratings. *Phys. Rev. B: Condens. Matter Mater. Phys.* **2016**, *93*, 155403.
(174) Messina, R.; Noto, A.; Guizal, B.; Antezza, M. Radiative heat transfer between metallic gratings using adaptive spatial resolution. *Phys. Rev. B: Condens. Matter Mater. Phys.* **2017**, *95*, 125404.
(175) Dai, J.; Dyakov, S. A.; Bozhevolnyi, S. I.; Yan, M. Near-field radiative heat transfer between metasurfaces: A full-wave study based on two-dimensional grooved metal plates. *Phys. Rev. B: Condens. Matter Mater. Phys.* **2016**, *94*, 125431.
(176) Pendry, J. B.; Martín-Moreno, L.; Garcia-Vidal, F. J. Mimicking surface plasmons with structured surfaces. *Science* **2004**, *305*, 847−848.
(177) Liu, X.; Zhao, B.; Zhang, Z. M. Enhanced near-field thermal radiation and reduced Casimir stiction between doped-Si gratings. *Phys. Rev. A: At., Mol., Opt. Phys.* **2015**, *91*, 062510.
(178) Liu, X.; Zhang, Z. M. Near-field thermal radiation between metasurfaces. *ACS Photonics* **2015**, *2*, 1320−1326.
(179) Fernández-Hurtado, V.; Garcia-Vidal, F. J.; Fan, S.; Cuevas, J. C. Enhancing near-field radiative heat transfer with Si-based metasurfaces. *Phys. Rev. Lett.* **2017**, *118*, 203901.
(180) Jin, W.; Molesky, S.; Lin, Z.; Rodriguez, A. W. Material scaling and frequency-selective enhancement of near-field radiative heat transfer for lossy metals in two dimensions via inverse design. 2018, arXiv:1802.05744 [physics.optics]. arXiv.org e-Print archive. https://arxiv.org/abs/1802.05744
(181) van Zwol, P. J.; Joulain, K.; Ben-Abdallah, P.; Chevrier, J. Phonon polaritons enhance near-field thermal transfer across the phase transition of VO_2. *Phys. Rev. B: Condens. Matter Mater. Phys.* **2011**, *84*, 161413.
(182) van Zwol, P. J.; Joulain, K.; Ben-Abdallah, P.; Greffet, J. J.; Chevrier, J. Fast nanoscale heat-flux modulation with phase-change materials. *Phys. Rev. B: Condens. Matter Mater. Phys.* **2011**, *83*, 201404.
(183) Cui, L. J.; Huang, Y.; Wang, J. Near-field radiative heat transfer between chiral metamaterials. *J. Appl. Phys.* **2012**, *112*, 084309.
(184) Huang, Y.; Boriskina, S. V.; Chen, G. Electrically tunable near-field radiative heat transfer via ferroelectric materials. *Appl. Phys. Lett.* **2014**, *105*, 244102.
(185) Moncada-Villa, E.; Fernández-Hurtado, V.; García-Vidal, F. J.; García-Martín, A.; Cuevas, J. C. Magnetic field control of near-field radiative heat transfer and the realization of highly tunable hyperbolic thermal emitters. *Phys. Rev. B: Condens. Matter Mater. Phys.* **2015**, *92*, 125418.
(186) Ben-Abdallah, P. Photon thermal Hall effect. *Phys. Rev. Lett.* **2016**, *116*, 084301.
(187) Zhu, L.; Fan, S. Persistent directional current at equilibrium in nonreciprocal many-body near field electromagnetic heat transfer. *Phys. Rev. Lett.* **2016**, *117*, 134303.
(188) Latella, I.; Ben-Abdallah, P. Giant thermal magnetoresistance in plasmonic structures. *Phys. Rev. Lett.* **2017**, *118*, 173902.
(189) Abraham Ekeroth, R. M.; Ben-Abdallah, P.; Cuevas, J. C.; García-Martín, A. Anisotropic thermal magnetoresistance for an active control of radiative heat transfer. *ACS Photonics* **2018**, *5*, 705−710.
(190) Basu, S.; Francoeur, M. Near-field radiative transfer based thermal rectification using doped silicon. *Appl. Phys. Lett.* **2011**, *98*, 113106.
(191) Iizuka, H.; Fan, S. H. Rectification of evanescent heat transfer between dielectric-coated and uncoated silicon carbide plates. *J. Appl. Phys.* **2012**, *112*, 024304.
(192) Wang, L. P.; Zhang, Z. M. Thermal rectification enabled by near-field radiative heat transfer between intrinsic silicon and a dissimilar material. *Nanoscale Microscale Thermophys. Eng.* **2013**, *17*, 337−348.
(193) Ben-Abdallah, P.; Biehs, S. A. Phase-change radiative thermal diode. *Appl. Phys. Lett.* **2013**, *103*, 191907.
(194) Yang, Y.; Basu, S.; Wang, L. P. Radiation-based near-field thermal rectification with phase transition materials. *Appl. Phys. Lett.* **2013**, *103*, 163101.
(195) Huang, J. G.; Li, Q.; Zheng, Z. H.; Xuan, Y. M. Thermal rectification based on thermochromic materials. *Int. J. Heat Mass Transfer* **2013**, *67*, 575−580.
(196) Nefzaoui, E.; Joulain, K.; Drevillon, J.; Ezzahri, Y. Radiative thermal rectification using superconducting materials. *Appl. Phys. Lett.* **2014**, *104*, 103905.
(197) Yang, Y.; Basu, S.; Wang, L. P. Vacuum thermal switch made of phase transition materials considering thin film and substrate effects. *J. Quant. Spectrosc. Radiat. Transfer* **2015**, *158*, 69−77.
(198) Ghanekar, A.; Ji, J.; Zheng, Y. High-rectification near-field thermal diode using phase change periodic nanostructure. *Appl. Phys. Lett.* **2016**, *109*, 123106.
(199) Zheng, Z. H.; Liu, X. L.; Wang, A.; Xuan, Y. M. Graphene-assisted near-field radiative thermal rectifier based on phase transition of vanadium dioxide (VO_2). *Int. J. Heat Mass Transfer* **2017**, *109*, 63−72.
(200) Ito, K.; Nishikawa, K.; Miura, A.; Toshiyoshi, H.; Iizuka, H. Dynamic modulation of radiative heat transfer beyond the blackbody limit. *Nano Lett.* **2017**, *17*, 4347−4353.
(201) Ito, K.; Nishikawa, K.; Iizuka, H.; Toshiyoshi, H. Experimental investigation of radiative thermal rectifier using vanadium dioxide. *Appl. Phys. Lett.* **2014**, *105*, 253503.
(202) Kubytskyi, V.; Biehs, S. A.; Ben-Abdallah, P. Radiative bistability and thermal memory. *Phys. Rev. Lett.* **2014**, *113*, 074301.
(203) Ben-Abdallah, P.; Biehs, S. A. Towards Boolean operations with thermal photons. *Phys. Rev. B: Condens. Matter Mater. Phys.* **2016**, *94*, 241401.
(204) Ben-Abdallah, P.; Biehs, S. A. Thermotronics: Towards nanocircuits to manage radiative heat flux. *Z. Naturforsch., A: Phys. Sci.* **2017**, *72*, 151−162.
(205) Würfel, P. The chemical potential of radiation. *J. Phys. C: Solid State Phys.* **1982**, *15*, 3967.

DOI: 10.1021/acsphotonics.8b01031
ACS Photonics 2018, 5, 3896−3915

(206) Berdahl, P. Radiant refrigeration by semiconductor diodes. *J. Appl. Phys.* **1985**, *58*, 1369.
(207) Liu, X.; Zhang, Z. M. High-performance electroluminescent refrigeration enabled by photon tunneling. *Nano Energy* **2016**, *26*, 353−359.
(208) Tervo, E.; Bagherisereshki, E.; Zhang, Z. Near-field radiative thermoelectric energy converters: a review. *Front. Energy* **2018**, *12*, 5−21.
(209) Shockley, W.; Queisser, H. J. Detailed balance limit of efficiency of p−n junction solar cells. *J. Appl. Phys.* **1961**, *32*, 510−519.
(210) Swanson, R. M. A proposed thermophotovoltaic solar energy conversion system. *Proc. IEEE* **1979**, *67*, 446−447.
(211) Fan, S. Photovoltaics: An alternative "Sun" for solar cells. *Nat. Nanotechnol.* **2014**, *9*, 92−93.
(212) Harder, N.-P.; Würfel, P. Theoretical limits of thermophotovoltaic solar energy conversion. *Semicond. Sci. Technol.* **2003**, *18*, S151−S157.
(213) DiMatteo, R. S.; Greiff, P.; Finberg, S. L.; Young-Waithe, K. A.; Choy, H. K. H.; Masaki, M. M.; Fonstad, C. G. Enhanced photogeneration of carriers in a semiconductor via coupling across a nonisothermal nanoscale vacuum gap. *Appl. Phys. Lett.* **2001**, *79*, 1894−1896.
(214) DiMatteo, R.; Greiff, P.; Seltzer, D.; Meulenberg, D.; Brown, E.; Carlen, E.; Kaiser, K.; Finberg, S.; Nguyen, H. Micron-gap ThermoPhotoVoltaics (MTPV). *AIP Conf. Proc.* **2004**, *738*, 42−51.
(215) Pralle, M. U.; Moelders, N.; McNeal, M. P.; Puscasu, I.; Greenwald, A. C.; Daly, J. T.; Johnson, E. A.; George, T.; Choi, D. S.; El-Kady, I.; Biswas, R. Photonic crystal enhanced narrow-band infrared emitters. *Appl. Phys. Lett.* **2002**, *81*, 4685−4687.
(216) Inoue, T.; De Zoysa, M.; Asano, T.; Noda, S. Single-peak narrow-bandwidth mid-infrared thermal emitters based on quantum wells and photonic crystals. *Appl. Phys. Lett.* **2013**, *102*, 191110.
(217) Inoue, T.; De Zoysa, M.; Asano, T.; Noda, S. High-Q mid-infrared thermal emitters operating with high power-utilization efficiency. *Opt. Express* **2016**, *24*, 15101−15109.
(218) Celanovic, I.; Perreault, D.; Kassakian, J. Resonant-cavity enhanced thermal emission. *Phys. Rev. B: Condens. Matter Mater. Phys.* **2005**, *72*, 075127.
(219) Dahan, N.; Niv, A.; Biener, G.; Gorodetski, Y.; Kleiner, V.; Hasman, E. Enhanced coherency of thermal emission: Beyond the limitation imposed by delocalized surface waves. *Phys. Rev. B: Condens. Matter Mater. Phys.* **2007**, *76*, 045427.
(220) Rephaeli, E.; Fan, S. Absorber and emitter for solar thermophotovoltaic systems to achieve efficiency exceeding the Shockley-Queisser limit. *Opt. Express* **2009**, *17*, 15145−15159.
(221) Maruyama, S.; Kashiwa, T.; Yugami, H.; Esashi, M. Thermal radiation from two-dimensionally confined modes in microcavities. *Appl. Phys. Lett.* **2001**, *79*, 1393−1395.
(222) Molesky, S.; Dewalt, C. J.; Jacob, Z. High temperature epsilon-near-zero and epsilon-near-pole metamaterial emitters for thermophotovoltaics. *Opt. Express* **2013**, *21*, A96−A110.
(223) Dyachenko, P. N.; Molesky, S.; Petrov, A. Y.; Störmer, M.; Krekeler, T.; Lang, S.; Ritter, M.; Jacob, Z.; Eich, M. Controlling thermal emission with refractory epsilon-near-zero metamaterials via topological transitions. *Nat. Commun.* **2016**, *7*, 11809.
(224) Yu, Z.; Sergeant, N. P.; Skauli, T.; Zhang, G.; Wang, H.; Fan, S. Enhancing far-field thermal emission with thermal extraction. *Nat. Commun.* **2013**, *4*, 1730.
(225) Simovski, C.; Maslovski, S.; Nefedov, I.; Kosulnikov, S.; Belov, P.; Tretyakov, S. Hyperlens makes thermal emission strongly super-Planckian. *Photonics Nanostructures* **2015**, *13*, 31−41.
(226) Miller, D. A. B.; Zhu, L.; Fan, S. Universal modal radiation laws for all thermal emitters. *Proc. Natl. Acad. Sci. U. S. A.* **2017**, *114*, 4336−4341.
(227) Greffet, J.-J.; Bouchon, P.; Brucoli, G.; Marquier, F. Light emission by nonequilibrium bodies: Local Kirchhoff law. *Phys. Rev. X* **2018**, *8*, 021008.
(228) Ilic, O.; Bermel, P.; Chen, G.; Joannopoulos, J. D.; Celanovic, I.; Soljačić, M. Tailoring high-temperature radiation and the resurrection of the incandescent source. *Nat. Nanotechnol.* **2016**, *11*, 320−324.
(229) Wuttke, C.; Rauschenbeutel, A. Thermalization via heat radiation of an individual object thinner than the thermal wavelength. *Phys. Rev. Lett.* **2013**, *111*, 024301.
(230) Kim, P.; Shi, L.; Majumdar, A.; McEuen, P. L. Thermal transport measurements of individual multiwall carbon nanotubes. *Phys. Rev. Lett.* **2001**, *87*, 215502.
(231) Shi, L.; Li, D.; Yu, C.; Jang, W.; Kim, D.; Yao, Z.; Kim, P.; Majumdar, A. Measuring thermal and thermoelectric properties of one-dimensional nanostructures using a microfabricated device. *J. Heat Transfer* **2003**, *125*, 881−888.
(232) Lee, S.; Yang, F.; Suh, J.; Yang, S.; Lee, Y.; Li, G.; Choe, H. S.; Suslu, A.; Chen, Y.; Ko, C.; Park, J.; Liu, K.; Li, J.; Hippalgaonkar, K.; Urban, J. J.; Tongay, S.; Wu, J. Anisotropic in-plane thermal conductivity of black phosphorus nanoribbons at temperatures higher than 100 K. *Nat. Commun.* **2015**, *6*, 8573.
(233) Lee, S.; Hippalgaonkar, K.; Yang, F.; Hong, J.; Ko, C.; Suh, J.; Liu, K.; Wang, K.; Urban, J. J.; Zhang, X.; Dames, C.; Hartnoll, S. A.; Delaire, O.; Wu, J. Anomalously low electronic thermal conductivity in metallic vanadium dioxide. *Science* **2017**, *355*, 371−374.
(234) Sadat, S.; Meyhofer, E.; Reddy, P. Resistance thermometry-based picowatt-resolution heat-flow calorimeters. *Appl. Phys. Lett.* **2013**, *102*, 163110.
(235) Zheng, J.; Wingert, M. C.; Dechaumphai, E.; Chen, R. Sub-picowatt/Kelvin resistive thermometry for probing nanoscale thermal transport. *Rev. Sci. Instrum.* **2013**, *84*, 114901.
(236) Thompson, D.; Zhu, L.; Mittapally, R.; Sadat, S.; Xing, Z.; McArdle, P.; Qazilbash, M. M.; Reddy, P.; Meyhofer, E. Hundred-fold enhancement in far-field radiative heat transfer over the blackbody limit. *Nature* **2018**, *561*, 216−221.
(237) Ben-Abdallah, P.; Biehs, S. A.; Joulain, K. Many-body radiative heat transfer theory. *Phys. Rev. Lett.* **2011**, *107*, 114301.
(238) Messina, R.; Antezza, M.; Ben-Abdallah, P. Three-body amplification of photon heat tunneling. *Phys. Rev. Lett.* **2012**, *109*, 244302.
(239) Ben-Abdallah, P.; Messina, R.; Biehs, S.-A.; Tschikin, M.; Joulain, K.; Henkel, C. Heat superdiffusion in plasmonic nanostructure networks. *Phys. Rev. Lett.* **2013**, *111*, 174301.
(240) Latella, I.; Biehs, S.-A.; Messina, R.; Rodriguez, A. W.; Ben-Abdallah, P. Ballistic near-field heat transport in dense many-body systems. *Phys. Rev. B: Condens. Matter Mater. Phys.* **2018**, *97*, 035423.
(241) Zhu, L.; Guo, Y.; Fan, S. Theory of many-body radiative heat transfer without the constraint of reciprocity. *Phys. Rev. B: Condens. Matter Mater. Phys.* **2018**, *97*, 094302.
(242) Volokitin, A. I.; Persson, B. N. J. Near-field radiative heat transfer between closely spaced graphene and amorphous SiO_2. *Phys. Rev. B: Condens. Matter Mater. Phys.* **2011**, *83*, 241407.
(243) Ilic, O.; Jablan, M.; Joannopoulos, J. D.; Celanovic, I.; Buljan, H.; Soljačić, M. Near-field thermal radiation transfer controlled by plasmons in graphene. *Phys. Rev. B: Condens. Matter Mater. Phys.* **2012**, *85*, 155422.
(244) Svetovoy, V. B.; van Zwol, P. J.; Chevrier, J. Plasmon enhanced near-field radiative heat transfer for graphene covered dielectrics. *Phys. Rev. B: Condens. Matter Mater. Phys.* **2012**, *85*, 155418.
(245) Lim, M.; Lee, S. S.; Lee, B. J. Near-field thermal radiation between graphene-covered doped silicon plates. *Opt. Express* **2013**, *21*, 22173−22185.
(246) Liu, X. L.; Zhang, Z. M. Graphene-assisted near-field radiative heat transfer between corrugated polar materials. *Appl. Phys. Lett.* **2014**, *104*, 251911.
(247) Messina, R.; Ben-Abdallah, P.; Guizal, B.; Antezza, M. Graphene-based amplification and tuning of near-field radiative heat transfer between dissimilar polar materials. *Phys. Rev. B: Condens. Matter Mater. Phys.* **2017**, *96*, 045402.

DOI: 10.1021/acsphotonics.8b01031
ACS Photonics 2018, 5, 3896−3915

(248) Liu, X. L.; Zhang, Z. M. Giant enhancement of nanoscale thermal radiation based on hyperbolic graphene plasmons. *Appl. Phys. Lett.* **2015**, *107*, 143114.
(249) Iizuka, H.; Fan, S. Analytical treatment of near-field electromagnetic heat transfer at the nanoscale. *Phys. Rev. B: Condens. Matter Mater. Phys.* **2015**, *92*, 144307.
(250) Ramirez, F. V.; Shen, S.; McGaughey, A. J. H. Near-field radiative heat transfer in graphene plasmonic nanodisk dimers. *Phys. Rev. B: Condens. Matter Mater. Phys.* **2017**, *96*, 165427.
(251) Yu, R.; Manjavacas, A.; García de Abajo, F. J. Ultrafast radiative heat transfer. *Nat. Commun.* **2017**, *8*, 2.
(252) Jin, W.; Polimeridis, A. G.; Rodriguez, A. W. Temperature control of thermal radiation from composite bodies. *Phys. Rev. B: Condens. Matter Mater. Phys.* **2016**, *93*, 121403.
(253) Miller, O. D.; Johnson, S. G.; Rodriguez, A. W. Shape-independent limits to near-field radiative heat transfer. *Phys. Rev. Lett.* **2015**, *115*, 204302.
(254) Hebestreit, E.; Reimann, R.; Frimmer, M.; Novotny, L. Measuring the internal temperature of a levitated nanoparticle in high vacuum. *Phys. Rev. A: At., Mol., Opt. Phys.* **2018**, *97*, 043803.
(255) Boriskina, S. V.; Zandavi, H.; Song, B.; Huang, Y.; Chen, Y. Heat is the new light. *Opt. Photonics News* **2017**, *28*, 26−33.

DOI: 10.1021/acsphotonics.8b01031
ACS Photonics 2018, 5, 3896−3915